PARAMETRIC STUDY AND DESIGN FORMULATION OF ALUMINIUM DAMPERS

A DISSERTATION

Submitted in partial fulfillment of the

requirements for the award of the degree

of

MASTER OF TECHNOLOGY

In

EARTHQUAKE ENGINEERING

(With Specialization in Structural dynamics)

by

P. S. R. S. PAVAN KUMAR

(Enrolment No-17526010)

DEPARTMENT OF EARTHQUAKE ENGINEERING

INDIAN INSTITUTE OF TECHNOLOGY ROORKEE

ROORKEE-247 667 (INDIA)

JUNE-2019

CANDIDATE'S DECLARATION

I **P. S. R. S. PAVAN KUMAR** hereby declare that the work presented in this dissertation entitled **"PARAMETRIC STUDY AND DESIGN FORMULATION OF ALUMINIUM DAMPERS",** in partial fulfillment of the requirement for the award of the degree in **Master of Technology** submitted to Department of Earthquake Engineering**,** Indian Institute of Technology Roorkee, India**,** under the supervision of

Dr. P. C. ASHWIN KUMAR (Assistant Professor)**.** It is an authentic record of my work done during the autumn semester of 2018-19 and spring semester of 2019-20. I have not submitted the matter embodied in this report for the award of any other degree.

Place: Roorkee P. S. R. S. PAVAN KUMAR

Date: Enrollment no. 17526010

CERTIFICATION

This is to certify that the above statement made by the candidate is correct to the best of my knowledge and belief.

Place: Roorkee (Dr. P. C. Ashwin Kumar)

Assistant Professor

Date: Department of Earthquake Engineering

Indian Institute of Technology Roorkee

ACKNOWLEDGEMENT

First appreciation goes to my parents, without whose beliefs, pursuing post-graduation would still have been a dream.

Completion of this dissertation would not have been possible without the expertise of my supervisor **Dr. P. C. Ashwin Kumar**, Assistant Professor in Department of Earthquake Engineering, Indian institute of Technology Roorkee. Frequent discussions throughout the dissertation work were extremely fruitful and helped me to overcome hurdles and problems I faced during this work.

Further, I would like to acknowledge the extremely good computer facilities provided by the department without which this work would not have been possible.

Scholarship given by Ministry of Human Resources and Development, Government of India is highly appreciated for this dissertation work.

Thanks to everyone who has helped me achieve this.

LIST OF CONTENTS

LIST OF FIGURES

LIST OF TABLES

ABSTRACT

The energy dissipation potential of a metallic damper depends mostly on the hysteretic response attained due to the inelastic deformation of plates under axial or flexural or shear loading. Mainly considering the metallic damper under shear loading, that is generated by the lateral loads of the structure. Shear panels yielding can be used to dissipate energy by hysteresis provided if the strength deterioration occurred by inelastic buckling is controlled. In the present study, the model is analytically examined 'cyclic inelastic buckling of aluminium panels in edge shear. 'Widely available aluminium alloy 6063, which is widely used for structural applications, was used as material of damper which is I-shaped specimens'. One hundred and fifty models of aluminium panels were generated with different geometric parameters, like web thickness, spacing of stiffeners, flange thickness, web length, web depth, stiffener thickness and number of panels which affect in the inelastic buckling. All the models were tested under reversed cyclic loading with increasing displacement levels. The buckling tendency of the panel is retarded on increasing web depth-to thickness ratio and reducing its aspect ratio. The models exhibited very ductile behaviour and very good energy dissipation potential with un-pinched and full hysteresis loops with shear strains up to 0.2 when element deletion value is 0.8 and shear strain up to 0.1 when element deletion value is 0.6 respectively. The analytical data set was used to acquire the proportionality factor in Gerard's formulation of inelastic buckling. The results are further used to obtain a relation between panel aspect ratio, the web panel depth-to-thickness ratio, and web buckling deformation angle for cyclic inelastic buckling, that can be used to determine the stiffener spacing, which limits the inelastic web buckling at design shear strains.

1 INTRODUCTION

For conventional concrete or steel structures, it is a reasonable way to increase the cross-section or reinforcement ratio to assure the seismic design requirements, such as load carrying capacity and the lateral drift ratio. However, if we adopt such seismic design we cannot really lower the seismic input and the seismic response of structures. Sadly, this greater cross section and reinforcement details will cause greater seismic energy input due to larger structural stiffness. When the structures are subjected to sudden and rare seismic loads, the seismic energy input will be dissipated with the help of plastic deformation in conventional seismic resistant structures.

So such seismic resistant structures will generally suffer great damage and large plastic deformation after the earthquake, leading the retrofit quite costly. Therefore, such approach cannot really improve much of the seismic performance of structures and also it makes the structures costly. In order to enhance the seismic behaviour of structures, recommendations such as energy-dissipation structures, devices and eccentrically braced frames were proposed in the 1970's and 1980's. These dissipate the seismic energy input by adding energy dissipation elements, decreasing the inter-story displacement of structures and internal force also avoiding failure in major members such as columns and shear walls. The key energy dissipation elements of eccentrically braced frames and energy dissipation structures are the metallic shear links and the metallic dampers, respectively. Therefore, the mechanical behaviour of the metallic shear links or the metallic dampers is critical.

The strength of metallic dampers is generally controlled by buckling. As of now dominantly steel and aluminium dampers are used in these applications, in which aluminium has Soft alloys that are less susceptible to web buckling problems because of their low yield strength which enables the usage of thicker webs.

The factors that majorly affect the buckling of aluminium plates are configuration/shape, loading type, fixity of the edges, type of alloy, etc. The purpose of this study is to analytically investigate the inelastic buckling behaviour of aluminium shear panels that can be used to provide the essential energy dissipation. Inelastic buckling of panels in shear, limits the energy dissipation potential of panels along with severe pinching of hysteresis loops. Therefore, shear panels are to be designed to avoid buckling at working shear strains. After the proportional limit the critical stresses given

by elastic buckling theory gives overestimate values, and in order to get acceptable results the behaviour of the material after the proportional limit must be considered. The modulus of elasticity, E, the slope of the stress-strain curve is the only mechanical property that effects the elastic buckling strength. In elastic range, *E* is constant, so slenderness ratio of the panel is the only parameter that governs the elastic buckling strength for a given alloy. Inelastic buckling occurs when the stress at the buckling stage is greater than the yield strength. The shear web buckling criteria of the Aluminium Association (2000) are primarily those reported by Clark and Rolf (1966). Sharp and Clark (1971) summarized the observed behaviour of thin aluminium shear webs of plate girders under monotonic loading which formed the basis of design provisions. Here, Gerard's approach (1948) is used for the inelastic buckling criterion which can be explicitly expressed in terms of applied cyclic shear strain, in order to use with deformation-based design provisions.

1.1 Inelastic buckling of aluminium panels in shear

The plate is said to be in 'pure shear' when it is subjected to edge shear stresses as shown in Figure1. Tensile and compressive stresses exist in the plate equal in magnitude to the shear stress with an inclined at 45º. The tendency to buckling caused by the compressive stresses is restrained by the tensile stresses. For elastic critical stress,

$$\tau_e = K_s \pi^2 \frac{E}{12(1-\mu^2)} \left(\frac{1}{\beta^2}\right) \tag{1.1}$$

Where

E = Young's Modulus

μ = Poisson's ratio

β = web depth- to-thickness ratio

k_s = buckling coefficient that is depending on aspect ratio α of the web sub panel formed by the transverse stiffeners and by its boundary restraint conditions. α can be defined as the ratio of stiffener spacing a to the clear depth of web ($d_w = d–2t_f$),

t_f = thickness of the flange and d is the overall depth of the panel.

The boundary conditions are clamped edge for the web panel, as the stiffeners are welded to flanges and web of the section providing significant restraint to the web.

For finite- length rectangular plate with clamped edges,

$$K_s = 8.98 + \frac{5.6}{\alpha^2},\ for(\alpha > 1) \tag{1.2}$$

$$K_s = 5.6 + \frac{8.98}{\alpha^2},\ for(\alpha \leq 1) \tag{1.3}$$

Since the inelastic critical stress lies beyond proportionality limit the tangent modulus of the material must be considered. If the material is following hook's law, now substitute the tangent modulus E_t in the Euler's buckling formula.

Now if the slenderness ratio is small the stress values follow tangent modulus curve and if the slenderness ratio is large, critical buckling stress values follow Euler's curve.

Inelastic buckling occurs when the stress at the buckling stage is greater than the proportional limit. At higher stresses where the inelastic buckling occurs then, tangent modulus or the slope of stress-strain curve must be replacing modulus of elasticity in Euler's buckling formula to find the inelastic buckling stress,

$$\tau_b = \left(\frac{\pi^2}{E_t \lambda^2}\right) \tag{1.4}$$

We can represent the inelastic buckling stress as a linear function of slenderness ratio λ as per Clark and Rolf (1966). Inelastic buckling stress,

$$\tau_b = B_S - D_S \tag{1.5}$$

Where B_s, D_s and C_s are from figure

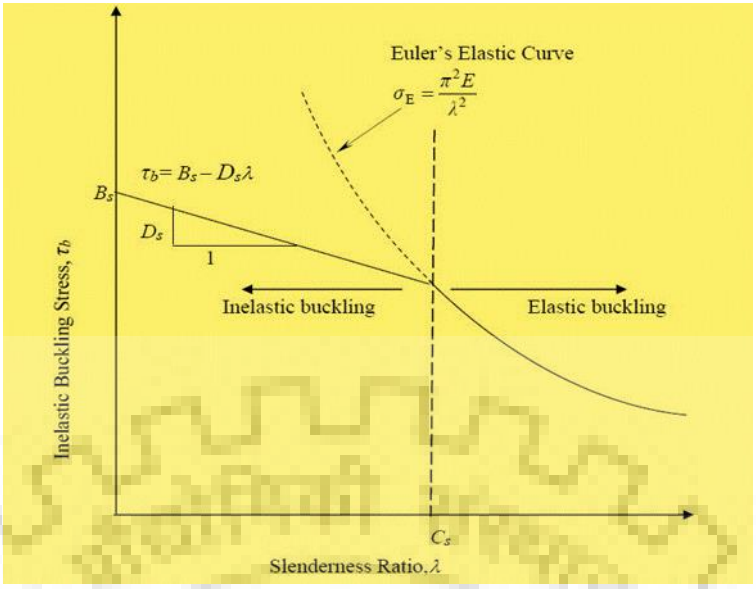

Figure 1.1 Buckling stress vs slenderness ratio

The straight line represents the inelastic buckling developed by aluminium plates. Formulas for B_s and D_s have been determined for aluminium alloys by Clark and Rolf (1966).

In ksi:

$$B_s = \tau_y \left[1 + \frac{\left(\tau_y^{\frac{1}{3}} \right)}{6.2} \right] \tag{1.6}$$

$$D_s = \frac{B_s}{20} \left[\frac{6B_s}{E} \right]^{(1/2)} \tag{1.7}$$

$$C_s = \frac{2B_s}{3D_s} \tag{1.8}$$

Where τ_y = yield stress in shear in ksi and

E = modulus of elasticity in ksi

In MPa:

$$B_s = \tau_y \left[1 + \frac{\left(\tau_y^{\frac{1}{3}} \right)}{11.88} \right] \tag{1.9}$$

$$D_s = \frac{B_s}{20}\left[\frac{6B_s}{E}\right]^{(1/2)} \quad (1.10)$$

$$C_s = \frac{2B_s}{3D_s} \quad (1.11)$$

Where τ_y= yield stress in shear in MPa and

E = modulus of elasticity in MPa

Gerard (1948) experimentally showed that if we stress the aluminium alloy plates beyond proportional limit in shear it shows same critical stress values if we use G_s/G ratio instead of E_t/E. Here G is the modulus in shear and G_s is the secant modulus in shear. G_s can be obtained from stress-strain diagram as ratio of $\frac{\tau}{\gamma}$ where τ = shear stress and γ = shear strain

1.2 Some applications of aluminium shear panels as EDDs

The energy dissipation devices (EDDs) are used mainly because they can easily be replaced after earthquake or dynamic loading. It also helps in preventing of the cumulation of the inelastic deformation in main load resisting members like beams, columns, etc. It also delocalises the damage induced in the structure.

The EDDs mainly absorb fraction of the input energy hence reducing energy dissipation demand of the structure and reduces the damage of the structure which increases scope for minimal retrofitting.

1.3 Energy dissipation devices (EDDs) are of four types:

1. **Viscous Dampers** (energy is absorbed by fluids present between piston cylindrical arrangement),

2. **Friction Dampers** (energy is absorbed due to presence of friction between surfaces),

3. **Yielding Dampers** (energy is absorbed by damping system by undergoing yielding).

4. **Visco-elastic Dampers** (energy is absorbed by utilizing the controlled shearing of solids).

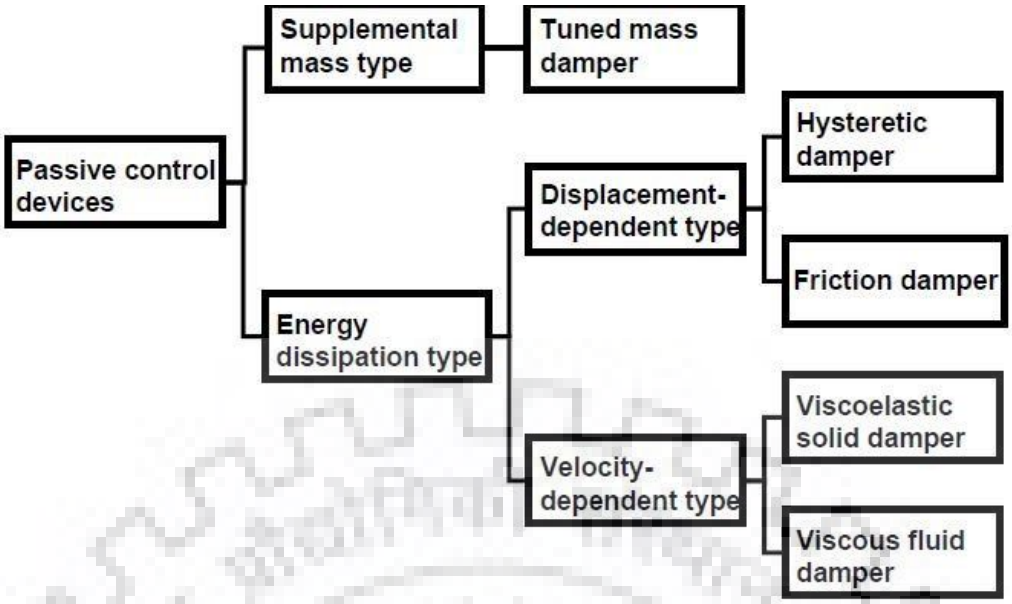

Figure 1.2 Flow chart of different type of passive control devices

Project is mainly concentrated on yielding dampers, as they provide energy dissipation through inelastic deformation.

The dampers are becoming popular in the construction of new building with higher resistance towards earthquakes and retrofitting of existing buildings. These can be installed easily in existing or new structures. Performance of a unit device or group of devices installed in a system or structure is of research interest now a days.

Best mechanism for the dissipation of energy of a structure is through the inelastic deformation of the metallic dampers. Dampers mainly resist the lateral forces which are Horizontal forces associated due to the inter-storey drift. Metallic dampers behaviour is controlled by geometric and mechanical parameters of metal that is used. At some increment of force the plates yield and thus provide an extra amount of energy dissipation. The energy dissipation demand of the main structure can be decreased by using aluminium shear panel as it behaves as a metallic damper which in turn dissipates the earthquake energy through the inelastic deformations.

These dampers can be used in improving the behavior of chevron type OCBF (Ordinary Concentric Braced Frames).

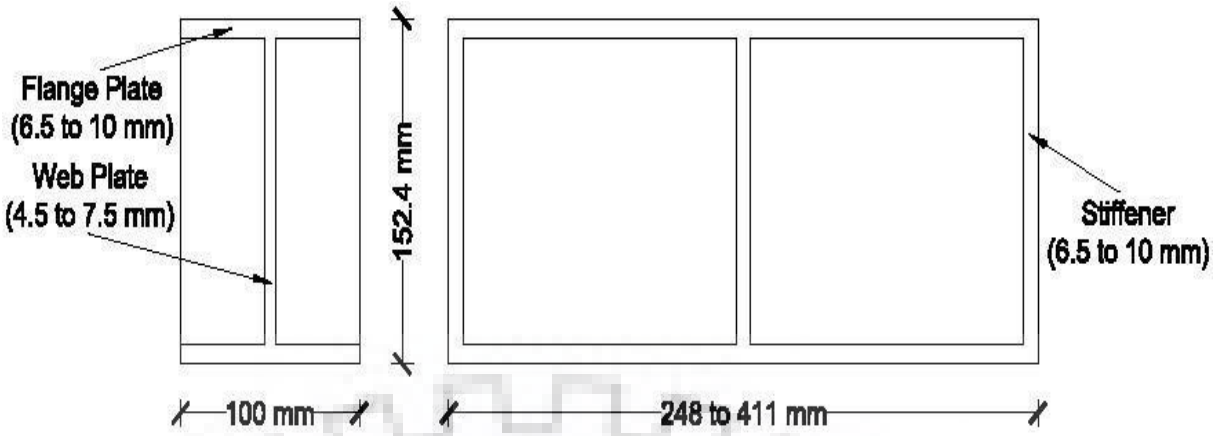

Figure 1.3 Aluminium shear link with 2 panels

An aluminium shear panel which is of I-section configuration can be introduced between end of diagonal braces and a beam of above floor, as shown below in figure1.4. The aluminium panel must be designed in such a way that it yields before the braces i.e the compression brace members buckle, so as to avoid the severe loss of strength and stiffness of the storey to buckling of the braces.

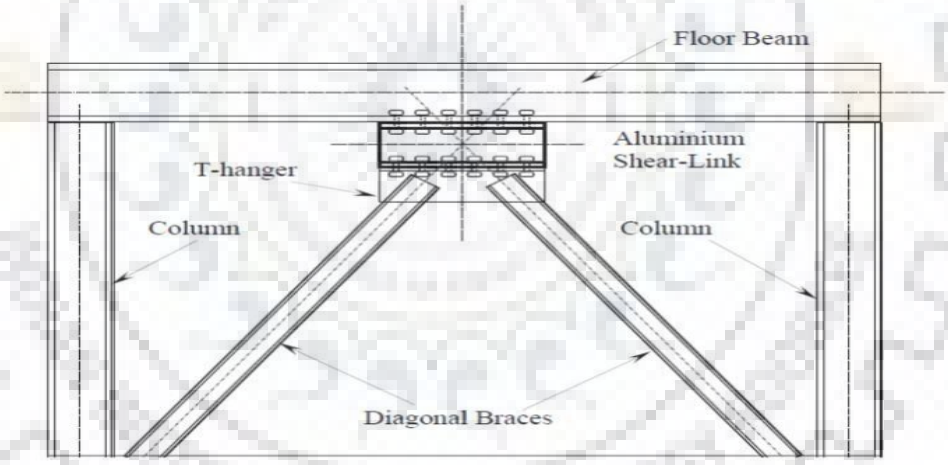

Figure 1.4 Schematic diagram of braced frame with aluminium shear panel (Rai, 1998)

With notable amount of strain hardening the aluminium allows the first critical link to yield and resist more lateral load which helps in absorbing the additional deformations by the dampers in the other storeys of a structure. This, strain hardening property of aluminium becomes an advantage to make all the dampers participate in the load dissipation which helps in avoiding the undesirable soft storey problem, which is a serious problem in the concentrated storey deformation (Rai and Wallace, 1998).

Truss Moment Frames (TMFs) are often used to span large open spaces in industrial and commercial buildings. So to enhance the seismic energy dissipation ability of the truss moment frames the Aluminium shear dampers can be used.Truss girder can be sorted in “K” or in a diamond shape “<>” and shear panels are placed in-between the horizontal vertices of braces of adjacent panels to withstand large plastic deformations. The aluminium shear dampers not only keep the stiffness of the diagonal members but also increase energy absorbing capacity though shear yielding of itself. The aluminium dampers safeguard the diagonal members from buckling and yielding also fails them when strong earthquake occurs. These dampers can easily be replaced. Figure 1.4 shows the arrangement of aluminium shear dampers in a TMF and its expected yield mechanism (Rai and Prasad, 1998).

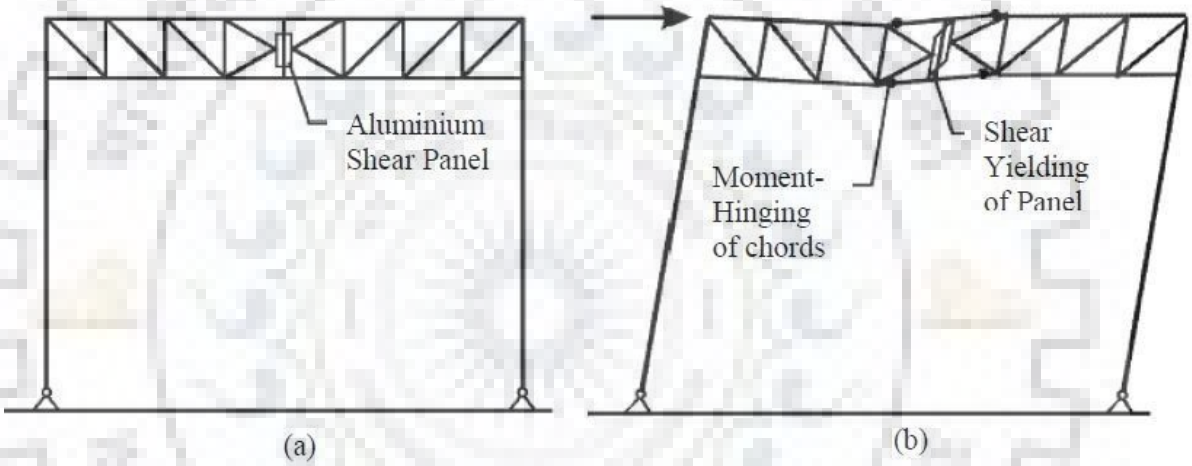

Figure 1.5 Typical arrangement of shear panel in Truss Moment Frame (b) Its collapse mechanism under lateral loads. (Rai, 1998)

2 LITERATURE REVIEW

Prerequisite data required for research has been obtained by reading different research papers. We can utilize the secant modulus for determining the critical stresses Gerard (1948). We must analytically determine the material constant that is to be used to find the critical shear stresses if the material exceeds proportionality constant. Critical-stress equation above proportional limit of material

$$\frac{\tau_{cr}}{\eta_s} = \frac{(2(1+\mu)K_S\pi^2 G)}{12(1-\mu^2)}\left(\frac{t}{b}\right)^2 \tag{2.1}$$

$$\tau_b = \eta(\tau)\tau_e \tag{2.2}$$

The material constant for shear instability above the proportional limit was proposed as $\eta(\tau) = \frac{G_s}{G}\tau_b$ is buckling stress, $\eta(\tau)$ is plastic-reduction factor which is dependent on the post elastic buckling behaviour of plate and is a function of shear modulus ratio as shown above equation, τ_e is the elastic buckling stress. $\eta(\tau)$ is function of the ratio of shear secant modulus *Gs* and shear modulus *G* of the shear panel as per Gerard (1948).

In terms of critical strain, $\gamma = \frac{\tau}{Gs}$ the above equation would be reduced to

$$\frac{\tau_{cr}}{G} = \frac{(2(1+\mu)Ks\pi^2\eta_s)}{12(1-\mu^2)}\left(\frac{t}{b}\right)^2 \tag{2.3}$$

Where t = panel thickness in inches, b = panel width in inches, and cr =critical (as subscript). Thus, Gerard developed these relations for monotonic loading. Kasai and Popov (1986) emphasized that shear links employed in eccentrically Braced Frames (EBFs) must be appropriately stiffened in order to prevent premature web buckling and retain energy dissipation capability. They conducted tests on various steel shear links and proposed criteria for web stiffener spacing as a function of inelastic cyclic shear link deformation based on secant modulus approach. They concluded that web buckling is the direct cause of link hysteretic behaviour deterioration. Buckling link deformation angle γ_b can be simply expressed in terms of aspect ratio and web depth to thickness ratio only and suggested that for post yield state

$$\frac{\tau_b}{\tau_e} = 1.85\frac{G_S}{G} \tag{2.4}$$

It is similar to Gerard's empirical plastic buckling solution relation utilizing the secant modulus as plastic reduction factor.

Clark and Rolf (1966) modified the tangent-modulus approach by a straight line equation for determining the shear buckling stress over the proportional limit.

Cyclic load tests on shear panel of low yield alloy of aluminium (3003-O) were performed by Rai (2002) to determine the onset and effect of inelastic web buckling on load-deformation behaviour. The author found Gerard's formulation for inelastic buckling, as reported in 1948 to be in excellent agreement with experimental results and used it to predict the onset of inelastic shear buckling to design shear panels so that inelastic buckling does not occur at strains below design requirements. Cyclic test on I shaped beams was used to obtain the proportionality factor in Gerard's formulation of inelastic buckling.

The author observed this factor to be nearly constant for all the specimens that were tested and indicated the proposed relation to be tentative as it was based on a very limited experimental data set.

It was suggested that in order to be definitive the data set must be expanded by indicating results from specimens of different geometries. The study using full scale models of shear panels using different geometric parameters has been taken up in the present research. Rai and Wallace (1998) conducted cyclic tests on medium scaled (1:4) models of aluminium shear links and studied their hysteretic behaviour and energy dissipation potential of two alloys of aluminium (3003-O) and (6061-O). These links were tested at different cyclic frequencies in order to determine the effect of strain rate. The links exhibited very ductile yielding in shear and a relatively small influence of strain rate was observed in the performance of the links. They also developed design equations to proportion these shear links, using data from cyclic load tests. They also designed a Shear-Link Brace Frame (SLBF) system and compared its seismic performance with that of an Ordinary Concentric Braced Frame (OCBF) with chevron braces. They concluded that SLBF system demonstrated more uniform storey drifts reduce base shear and, a larger energy dissipation capacity per unit drift. Rai and Wallace (2000) designed aluminium beam to yield in shear to limit the maximum force due to lateral load transmitted to the primary structural members. They observed that the shear yielding of aluminium is very ductile and large inelastic deformations (about

10% strains) are possible without tearing. They also conducted numerical studies to show the effectiveness of aluminium shear links for Concentric Braced Frames (CBFs) and Truss Moment Frames (TMFs). Rai and Prasad (1998) developed a methodology to design a Truss.

Moment Frame (TMF) with shear link as energy dissipator. They compared the seismic performance of Shear-Link TMF with Special Truss Moment Frame (SMTF) for various ground motions. They found Shear-Link TMF demonstrated reduced energy input, base shear, storey drift and a larger energy dissipation capacity per unit drift. Rai (2001) emphasized the need for slow cyclic testing for evaluation of seismic performance of structural components to bridge the gap between the "expected" and the "observed" behaviour. The author described the experimental test program of shear link as evaluation of an energy dissipation device as an example. The modeling process, testing system, instrumentation, data acquisition and loading history in a case study has also been described.

Developments in the field of earthquake-resistant design of structures were presented by Rai (2000). The author favoured the strategy for enhancing seismic performance of fixed-base systems involving dissipation of seismic energy through various Energy Dissipation Devices (EDDs). The author discussed techniques that used materials such as steel, aluminium and placing them strategically to modify the force deformation response of structural components and thus enhance their energy dissipation potential.

2.1 Temper Designations

In aluminium alloys, the mechanical properties may be changed by heat treatment. Heat is used to enhance strength but can also be used to decrease strength through annealing to assist with forming; these alloys can also be re-heat-treated after annealing or forming to restore their original properties.

There are 3 basic temper groupings for aluminium products:

"O" - Dead soft (i.e. fully annealed)

"T" - Heat treated (i.e. for age hardening alloys)

"H" - Strain hardened (i.e. for non-age hardening alloys)

2.2 Annealing Process

Annealing is a softening process where the steel is heated to the austenitic or austenite-cementitite temperatures and then slowly cooled. Annealing is commonly used to soften materials and minimize residual stresses, improve machinability, and increase ductility by carefully controlling the microstructure. The specimens were annealed and stress-relieved before the experiment. They were raised to a temperature of 420 degree C and kept at that temperature for two hours. Then they were allowed to cool gradually at a rate of 30 degree C per hour in the heat treating oven.

2.3 Effect of annealing

Annealing resulted in the reduction in the values of yield stress and ultimate stress of aluminium. It has been observed that due to annealing, the reduction in the yield stress of aluminium was much more pronounced than the reduction in ultimate stress as described in Fig 2.4. Thus, unannealed tensile coupon tests result in a curve with a sharp knee, and the stress-strain curve of annealed coupons is more rounded with much lower yield stress. Thus it can be concluded that after annealing, the strain-hardening of the material increases.

As stated earlier, the objective of this study is to understand the force-deformation behaviour of the shear links under slow cyclic loading. “Slow cyclic” implies that load or deformation cycles are imposed on a test specimen in a slow, controlled and predetermined manner, and dynamic effects as well as rate of deformation effects are not considered. Therefore, the specimens were subjected to cyclic loading in displacement controlled regimes. One of the most important points in slow cyclic tests was the type of loading history to be used. In the present study, a simple multi-step loading history based on ATC-24 (1992) guidelines was applied.

2.4 OBJECTIVE

- The objective of this study is to investigate the inelastic buckling of aluminium panels in shear analytically by modelling in Abaqus software.
- Parametric study of the inelastic behaviour of aluminium shear panels is to be carried out. Aluminium 6063-O alloy is used and damper shaped as I section are modelled and are tested analytically under cyclic loading condition through the increasing displacement levels. Shear damper shaped as a I section had geometric parameters such as web thickness, ratio of interior stiffeners to that of exterior stiffeners, web depth-to-thickness ratio, aspect ratio of panels, ratio of flange plate thickness to web thickness, number of panels. These parameters are varied one by one keeping the remaining parameters same for all the specimens.

As stated earlier, the objective is to keenly understand the force-deformation behavior of the shear links imposed by slow cyclic loading. If the load or deformation cycles on the test specimen are imposed slowly in a controlled and predetermined manner and by excluding the dynamic effects and deformation effects is called "Slow cyclic loading". This explains that the specimens were undergone through the cyclic loading in displacement controlled regimes. The most important to be noted is the type of loading history to be considered so as to input in the software for the analysis. A simple multi-step loading history based on ATC-24 (1992) guidelines has been applied in the following parametric study and for the validation of the model with the specimen used in Jain *et al.* (2008). The analysis are done to produce basic information on the aluminium shear panel behaviour including data on strength and stiffness characteristics, deformation capacities, cyclic strain hardening effects, and deterioration behaviour at large deformations.

- The present study is to acquire as much as of this information as feasible. Buckling of the panel seems to be an acceptable criterion for the design consideration of aluminium panels in shear because after buckling of panel, pinching of hysteresis loops occur resulting in reduction in energy dissipation potential. The geometric parameters that determine buckling of the shear panel are the web thickness t_w, clear web depth d_w, between the flanges, the spacing a of the transverse stiffeners, thickness of the stiffeners and many other parameters.

- Design provisions will be proposed based on Gerard's formulation of inelastic buckling. The experimental data set was used to obtain the proportionality factor in Gerard's formulation of inelastic buckling.
- This result is further used to obtain a relation between panel aspect ratio, the web panel depth-to-thickness ratio, and web buckling deformation angle for cyclic inelastic buckling, which can be used to determine the spacing of stiffeners, which will limit the inelastic web buckling at design shear strains. Analysing the hysteresis behaviour of the damper under edge shear force. Also comparison of performance of aluminium with the performance of steel for the given shear force.

3 NUMERICAL MODELLING IN ABAQUS

I-section as damper: In absence of earthquake the I-section provides extra factor of safety towards the resisting of the dead load of the building**.** The shear link is developed in Abaqus using shell type. Later the main web panel the flange panels and the stiffeners are developed differently and given an interaction at the later stage.

Then the following material details as shown in below table are used to generate the aluminium model. Material properties used in abaqus modelling, validation and parametric study is basically Aluminium 6063-O which is a ductile variety of material with Youngs modulus and Poisson's ratio as below:

Table 3.1 Engineering properties of aluminium 6063-O

Young's modulus	Poisson's ratio
16.88 x 10^9 N/m^2	0.33

Table 3.2 The typical properties for aluminium

Property	Value
Melting Point (°C)	660
Boiling Point (°C)	2480
Mean Specific Heat (0 -100°C)(calorie/g.°C)	0.219
Thermal Conductivity (0-100°C)(calorie/cms. °C)	0.57
Co-Efficient of Linear Expansion(0-100°C) (x10^{-6}/°C)	23.5
Electrical Resistivity (μΩcm)	2.69
Density (g/cc)	2.7
Modulus of Elasticity (GPa)	68.3
Poisson's Ratio	0.34

Table 3.3 Engineering properties

Alloy	Condition	%Elongation	Yield stress MPa	Ultimate stress MPa
6063-O	Annealed	31.08	35	85

The slow loading rate as described in the previous chapter is followed and this loading protocol follows three cycles each of ± 0.005, 0.01, 0.02, 0.05, 0.10, 0.15, 0.20 and 0.25 strain.

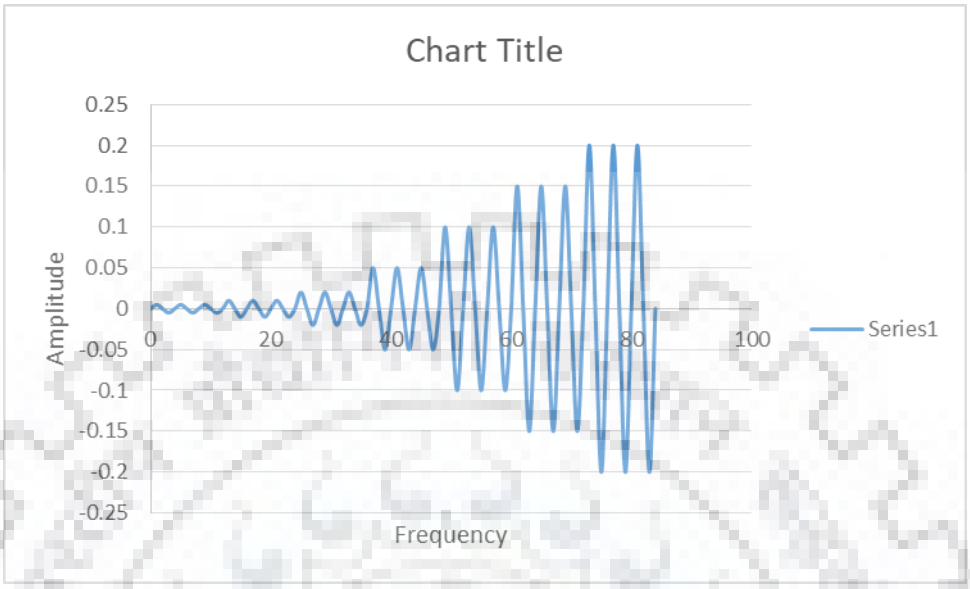

Figure 3.1 Loading protocol as per ATC-24 (1992)

The model of damper is divided into 3 components namely flanges, web panel, stiffeners (end stiffeners, intermediate stiffeners).

Shell type of modelling is chosen. The model is made depending on the number of panels namely one, two, three panel damper. As shown in the figure.

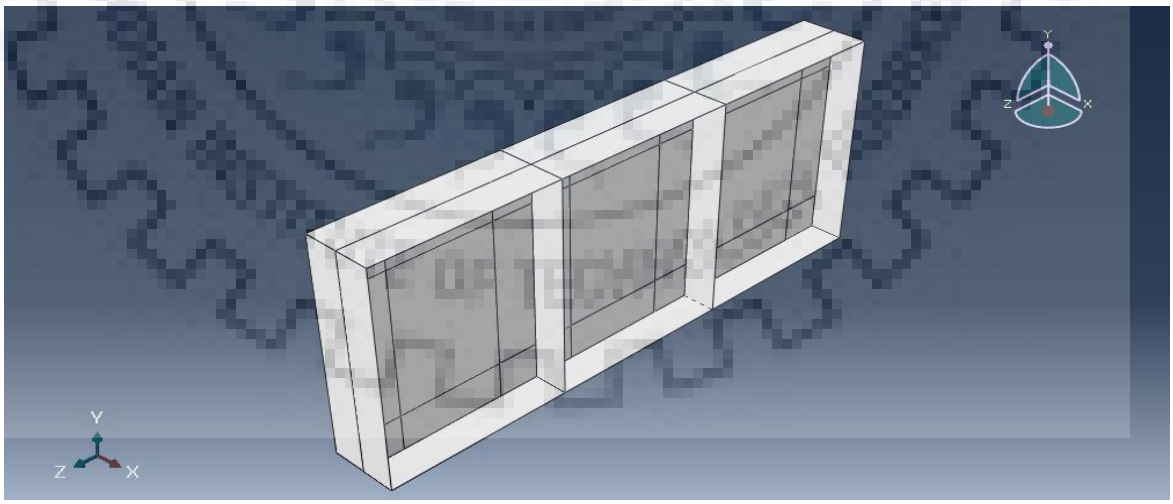

Figure 3.2 Typical model of three panels generated in Abaqus

Element type and mesh pattern used are S4R as described in some papers who worked on different material like steel, papers namely

Sjain (2008) and Jian-Sheng Fan (2017) and are shown in figure

The interaction details used in the model are MPC by defining a reference point so as to idealise the behavior during the loading.

Later the end conditions are defined in such a way that the damper is confined to move in y direction so as to restrain its behavior such that the web panel fails due to out of plane buckling which is the criteria required to observe the remaining parameters and design values as per Gerard's approach.

By element type**:** S4R quadrilateral linear 28360

By part: Flange+Web+Stiffener elements= 28360 no of nodes= 28584

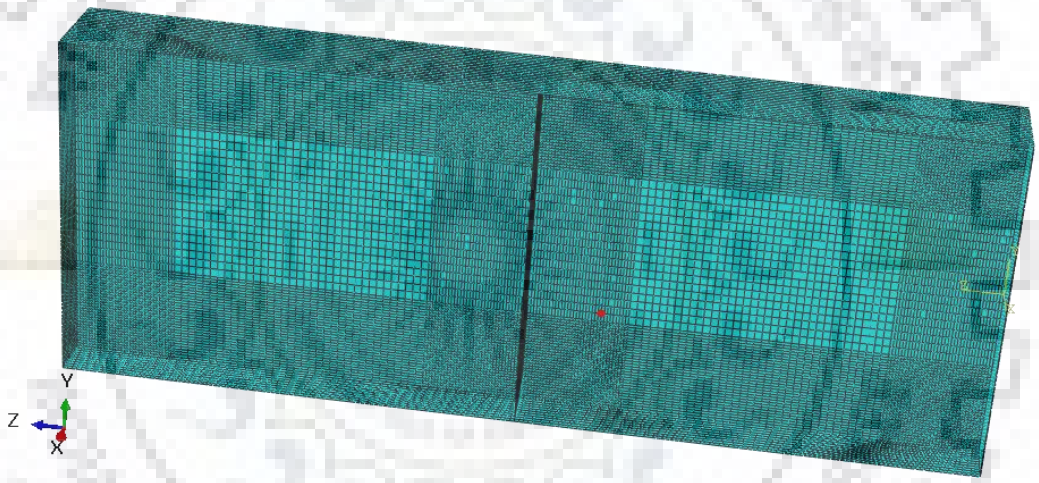

Figure 3.3 Meshing details

After the generation of the model the model is run using the above conditions and some extra parameters like the increment size mesh size etc. the following diagram shows the model after the analysis with the dimension of the model data I4 as defined by me in the table.

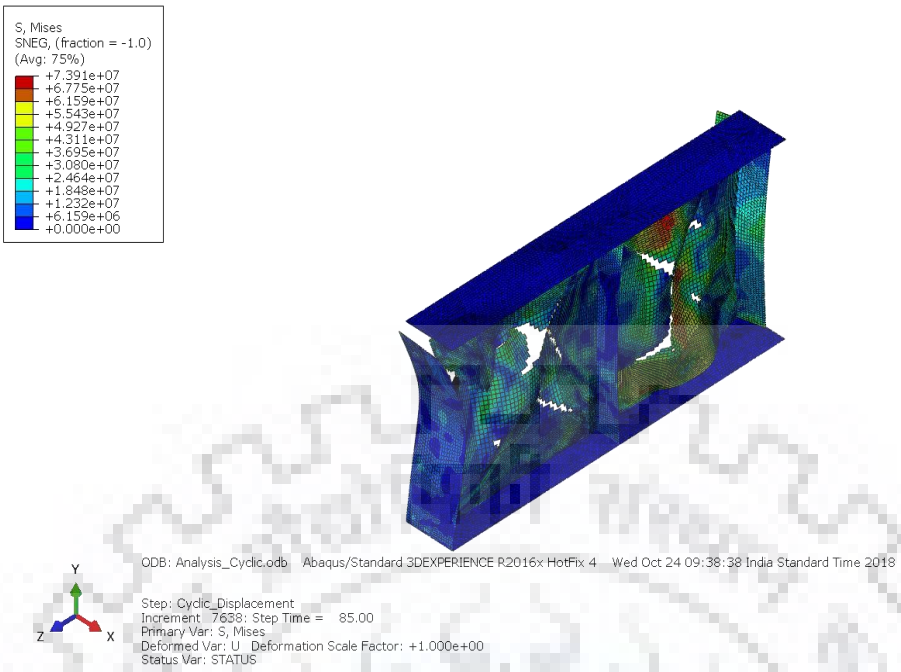

Figure 3.4 Figure of model I3 after running analysis showing the failure pattern

4 MODELLING VALIDATION

Constraints used are bottom, top flange MPC (multiple point constraint). Model has been validated with the element deletion factor as .82 with S. JAIN experimental data as given in paper Jain *et al.* (2008) and the results are found to be satisfactory as shown below in figure.

Table 4.1 The dimensions of the specimen taken from S. Jain journal paper for validation of Abaqus model.

Specimen No.	No. of panels	t_w (mm)	Clear spacing of stiffeners (mm)	α	Thickness ratio	Length of web (mm)	Area of web A_w (mm^2)	t_s (mm)
2	2	4.5	114.3	0.75	38.1	248.1	1116.45	6.5
5	3	4.5	114.3	0.75	38.1	368.9	1660.05	6.5

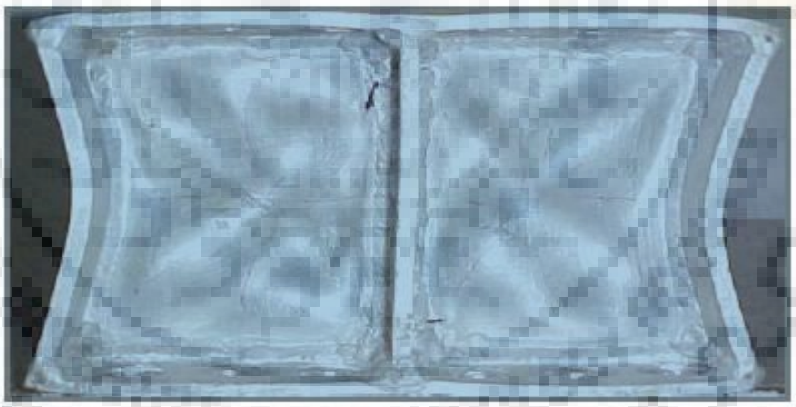

Figure 4.1 Specimen 2 buckled at 0.10 strain, failure due to tearing of web plate at corners Jain *et al*. (2008)

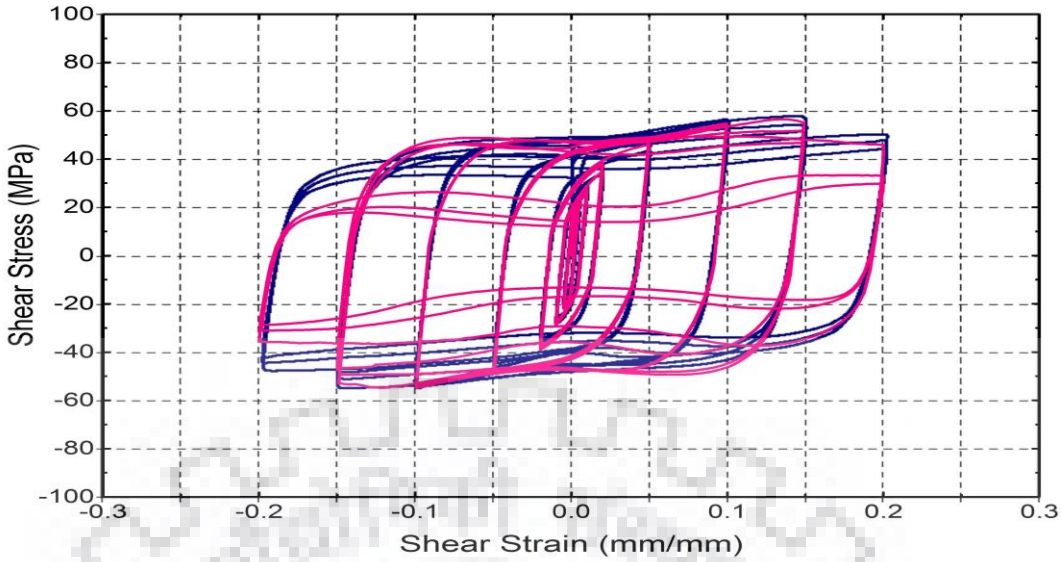

Figure 4.2 Specimen 2 validation from Jain *et al*. (2008) experimental data

Figure 4.3 Photo of specimen 5 tested by Jain *et al.* (2008).

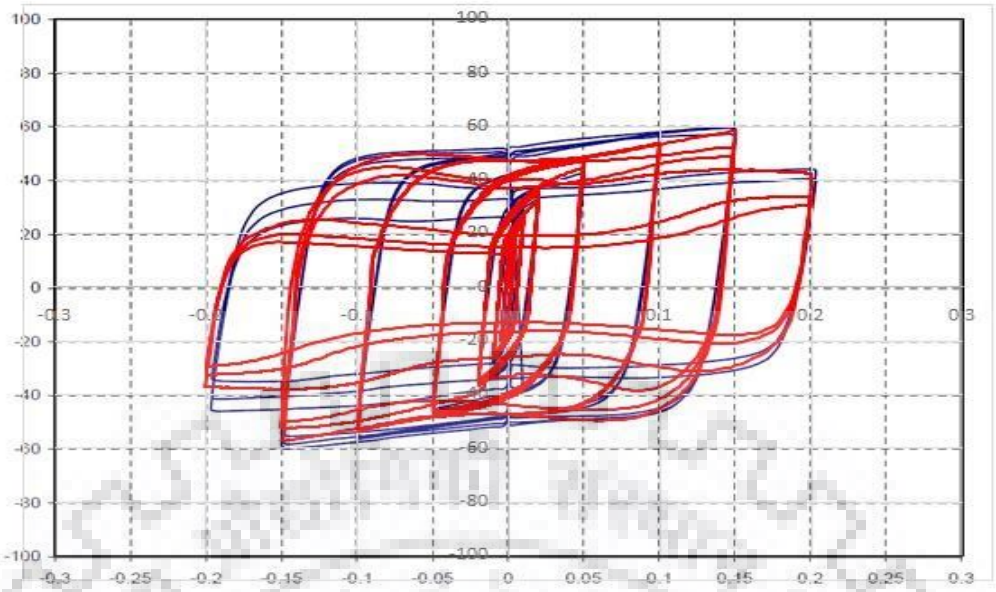

Figure 4.4 Specimen 5 validation from Jain *et al*. (2008) experimental data

Since the available experimental test results are showing a good agreement with the analytical model generated results, which paved me a way to proceeded forward with my parametric study. The parametric study is carried out with the models generated on the basis of the parametric table 4.1 as shown below.

5 PARAMETRIC STUDY

The idea of the parametric study is obtained from Sachin Jain experimental work on the aluminium shear panels. He has taken 19 specimens only with 2 panels and 3 panels varying the web thickness and web length of the specimen and taking only 2 α values 0.75 and 1.25 respectively and taken the thickness of web as 4.5mm, 6.5mm, and 7.6mm only.

Out of his experimentation he has obtained 7 out of 19 results which has never reached the inelastic buckling state and some showed internal failures so there is a need to study the behaviour of the parameters in a larger set of values varying as many parameters as possible so as to jump to a conclusion with a proof of a larger set of design values namely the inelastic buckling stress elastic buckling stress mainly the factor correlating the inelastic and elastic buckling stress which is the proportionality factor as per Gerard's formulation for shear dampers. In this parametric study we have varied a large number of parameters and the larger number of samples nearly 150 models varying parameters namely the panel aspect ratio α, the web depth to thickness ratio β,number of panels, thickness of stiffeners, thickness of flange etc. So the following observations are made from the results obtained from Abaqus and Matlab (energy curves generation) the energy curves are the extra result that helps us to gain a view of the point at which inelastic buckling has occurred and the energy that is there after the inelastic buckling .

Table 5.1 Showing all the parameters that have been varied

Name	Width of flange	Clear depth of web	Total length of web	α	Clear spacing between stiff	Thick-ness of web	β	Thickness of end stiffener	Thickness of intermediate stiffener	Thickness of flange	Number of panels	t_w/t_s	t_w/t_f
A1	100	350	215	0.5	175	10	35	20	0	20	1	0.5	0.5
A2	100	350	302.5	0.75	262.5	10	35	20	0	20	1	0.5	0.5
A3	100	350	390	1	350	10	35	20	0	20	1	0.5	0.5
A4	100	350	477.5	1.25	437.5	10	35	20	0	20	1	0.5	0.5
A5	100	350	565	1.5	525	10	35	20	0	20	1	0.5	0.5
A6	100	350	740	2	700	10	35	20	0	20	1	0.5	0.5
B1	100	350	410	0.5	175	10	35	20	20	20	2	0.5	0.5
B2	100	350	585	0.75	262.5	10	35	20	20	20	2	0.5	0.5
B3	100	350	760	1	350	10	35	20	20	20	2	0.5	0.5
B4	100	350	935	1.25	437.5	10	35	20	20	20	2	0.5	0.5
B5	100	350	1110	1.5	525	10	35	20	20	20	2	0.5	0.5

Name	Width of flange	Clear depth of web	Total length of web	α	Clear spacing between stiff	Thick-ness of web	β	Thickness of end stiffener	Thickness of intermediate stiffener	Thickness of flange	Number of panels	t_w/t_s	t_w/t_f
B6	100	350	1460	2	700	10	35	20	20	20	2	0.5	0.5
C1	100	350	605	0.5	175	10	35	20	20	20	3	0.5	0.5
C2	100	350	867.5	0.75	262.5	10	35	20	20	20	3	0.5	0.5
C3	100	350	1130	1	350	10	35	20	20	20	3	0.5	0.5
C4	100	350	1392.5	1.25	437.5	10	35	20	20	20	3	0.5	0.5
C5	100	350	1655	1.5	525	10	35	20	20	20	3	0.5	0.5
C6	100	350	2180	2	700	10	35	20	20	20	3	0.5	0.5
D1	100	350	195	0.5	175	5	70	10	0	5	1		1
D2	100	350	282.5	0.75	262.5	5	70	10	0	5	1		1
D3	100	350	370	1	350	5	70	10	0	5	1		1
D4	100	350	457.5	1.25	437.5	5	70	10	0	5	1		1
D5	100	350	545	1.5	525	5	70	10	0	5	1		1

Name	Width of flange	Clear depth of web	Total length of web	α	Clear spacing between stiff	Thick-ness of web	β	Thickness of end stiffener	Thickness of intermediate stiffener	Thickness of flange	Number of panels	t_w/t_s	t_w/t_f
D6	100	350	720	2	700	5	70	10	0	5	1		1
E1	100	350	275	0.5	175	25	14	50	0	25	1		1
E2	100	350	362.5	0.75	262.5	25	14	50	0	25	1		1
E3	100	350	450	1	350	25	14	50	0	25	1		1
E4	100	350	537.5	1.25	437.5	25	14	50	0	25	1		1
E5	100	350	625	1.5	525	25	14	50	0	25	1		1
E6	100	350	800	2	700	25	14	50	0	25	1		1
F1	100	350	315	0.5	175	35	10	70	0	70	1	0.5	0.5
F2	100	350	402.5	0.75	262.5	35	10	70	0	70	1	0.5	0.5
F3	100	350	490	1	350	35	10	70	0	70	1	0.5	0.5
F4	100	350	577.5	1.25	437.5	35	10	70	0	70	1	0.5	0.5
F5	100	350	665	1.5	525	35	10	70	0	70	1	0.5	0.5

Name	Width of flange	Clear depth of web	Total length of web	α	Clear spacing between stiff	Thick-ness of web	β	Thickness of end stiffener	Thickness of intermediate stiffener	Thickness of flange	Number of panels	t_w/t_s	t_w/t_f
F6	100	350	840	2	700	35	10	70	0	70	1	0.5	0.5
G4	100	350	493.5	1.25	437.5	14	25	28	0	28	1	0.5	0.5
G5	100	350	581	1.5	525	14	25	28	0	28	1	0.5	0.5
G6	100	350	756	2	700	14	25	28	0	28	1	0.5	0.5
H1	100	350	245	0.5	175	17.5	20	35	0	35	1	0.5	0.5
H2	100	350	332.5	0.75	262.5	17.5	20	35	0	35	1	0.5	0.5
H3	100	350	420	1	350	17.5	20	35	0	35	1	0.5	0.5
H4	100	350	507.5	1.25	437.5	17.5	20	35	0	35	1	0.5	0.5
1H4	100	350	507.5	1.25	437.5	17.5	20	35	0	17.5	1	0.5	1
H5	100	350	595	1.5	525	17.5	20	35	0	35	1	0.5	0.5
H6	100	350	770	2	700	17.5	20	35	0	35	1	0.5	0.5
I1	100	350	380	0.5	175	5	70	10	10	10	2	0.5	0.5

Name	Width of flange	Clear depth of web	Total length of web	α	Clear spacing between stiff	Thick-ness of web	β	Thickness of end stiffener	Thickness of intermediate stiffener	Thickness of flange	Number of panels	t_w/t_s	t_w/t_f
I2	100	350	555	0.75	262.5	5	70	10	10	10	2	0.5	0.5
I3	100	350	730	1	350	5	70	10	10	10	2	0.5	0.5
I4	100	350	905	1.25	437.5	5	70	10	10	10	2	0.5	0.5
I5	100	350	1080	1.5	525	5	70	10	10	10	2	0.5	0.5
I6	100	350	1430	2	700	5	70	10	10	10	2	0.5	0.5
J1	100	350	500	0.5	175	25	14	50	50	50	2	0.5	0.5
J2	100	350	675	0.75	262.5	25	14	50	50	50	2	0.5	0.5
J3	100	350	850	1	350	25	14	50	50	50	2	0.5	0.5
J4	100	350	1025	1.25	437.5	25	14	50	50	50	2	0.5	0.5
J5	100	350	1200	1.5	525	25	14	50	50	50	2	0.5	0.5
J6	100	350	1550	2	700	25	14	50	50	50	2	0.5	0.5
K1	100	350	560	0.5	175	35	10	70	70	70	2	0.5	0.5

Name	Width of flange	Clear depth of web	Total length of web	α	Clear spacing between stiff	Thick-ness of web	β	Thickness of end stiffener	Thickness of intermediate stiffener	Thickness of flange	Number of panels	t_w/t_s	t_w/t_f
K2	100	350	735	0.75	262.5	35	10	70	70	70	2	0.5	0.5
K3	100	350	910	1	350	35	10	70	70	70	2	0.5	0.5
K4	100	350	1085	1.25	437.5	35	10	70	70	70	2	0.5	0.5
K5	100	350	1260	1.5	525	35	10	70	70	70	2	0.5	0.5
K6	100	350	1610	2	700	35	10	70	70	70	2	0.5	0.5
L1	100	350	434	0.5	175	14	25	28	28	28	2	0.5	0.5
L3	100	350	784	1	350	14	25	28	28	28	2	0.5	0.5
L4	100	350	959	1.25	437.5	14	25	28	28	28	2	0.5	0.5
L5	100	350	1134	1.5	525	14	25	28	28	28	2	0.5	0.5
L6	100	350	1484	2	700	14	25	28	28	28	2	0.5	0.5
M1	100	350	455	0.5	175	17.5	20	35	35	35	2	0.5	0.5
M2	100	350	630	0.75	262.5	17.5	20	35	35	35	2	0.5	0.5

Name	Width of flange	Clear depth of web	Total length of web	α	Clear spacing between stiff	Thick-ness of web	β	Thickness of end stiffener	Thickness of intermediate stiffener	Thickness of flange	Number of panels	t_w/t_s	t_w/t_f
M3	100	350	805	1	350	17.5	20	35	35	35	2	0.5	0.5
M4	100	350	980	1.25	437.5	17.5	20	35	35	35	2	0.5	0.5
M5	100	350	1155	1.5	525	17.5	20	35	35	35	2	0.5	0.5
M6	100	350	1505	2	700	17.5	20	35	35	35	2	0.5	0.5
N1	100	350	565	0.5	175	5	70	10	10	10	3	0.5	0.5
N2	100	350	827.5	0.75	262.5	5	70	10	10	10	3	0.5	0.5
N3	100	350	1090	1	350	5	70	10	10	10	3	0.5	0.5
N4	100	350	1352.5	1.25	437.5	5	70	10	10	10	3	0.5	0.5
O1	100	350	725	0.5	175	25	14	50	50	50	3	0.5	0.5
O2	100	350	987.5	0.75	262.5	25	14	50	50	50	3	0.5	0.5
O3	100	350	1250	1	350	25	14	50	50	50	3	0.5	0.5
O4	100	350	1512.5	1.25	437.5	25	14	50	50	50	3	0.5	0.5

Name	Width of flange	Clear depth of web	Total length of web	α	Clear spacing between stiff	Thick-ness of web	β	Thickness of end stiffener	Thickness of intermediate stiffener	Thickness of flange	Number of panels	t_w/t_s	t_w/t_f
P1	100	350	805	0.5	175	35	10	70	70	70	3	0.5	0.5
P2	100	350	1067.5	0.75	262.5	35	10	70	70	70	3	0.5	0.5
P3	100	350	1330	1	350	35	10	70	70	70	3	0.5	0.5
P4	100	350	1592.5	1.25	437.5	35	10	70	70	70	3	0.5	0.5
Q1	100	350	637	0.5	175	14	25	28	28	28	3	0.5	0.5
Q2	100	350	899.5	0.75	262.5	14	25	28	28	28	3	0.5	0.5
Q3	100	350	1162	1	350	14	25	28	28	28	3	0.5	0.5
Q4	100	350	1424.5	1.25	437.5	14	25	28	28	28	3	0.5	0.5
R1	100	350	665	0.5	175	17.5	20	35	35	35	3	0.5	0.5
R2	100	350	927.5	0.75	262.5	17.5	20	35	35	35	3	0.5	0.5
R3	100	350	1190	1	350	17.5	20	35	35	35	3	0.5	0.5
R4	100	350	1452.5	1.25	437.5	17.5	20	35	35	35	3	0.5	0.5

5.1 Observation of the behavior of damper when we vary only α

Table 5.2 Showing the dimensions taken in the model A

Name	b_f	d_w	C	α	t_w	β	t_s
A1	100	350	175	0.5	10	35	20
A2	100	350	262.5	0.75	10	35	20
A3	100	350	350	1	10	35	20
A4	100	350	437.5	1.25	10	35	20
A5	100	350	525	1.5	10	35	20
A6	100	350	700	2	10	35	20

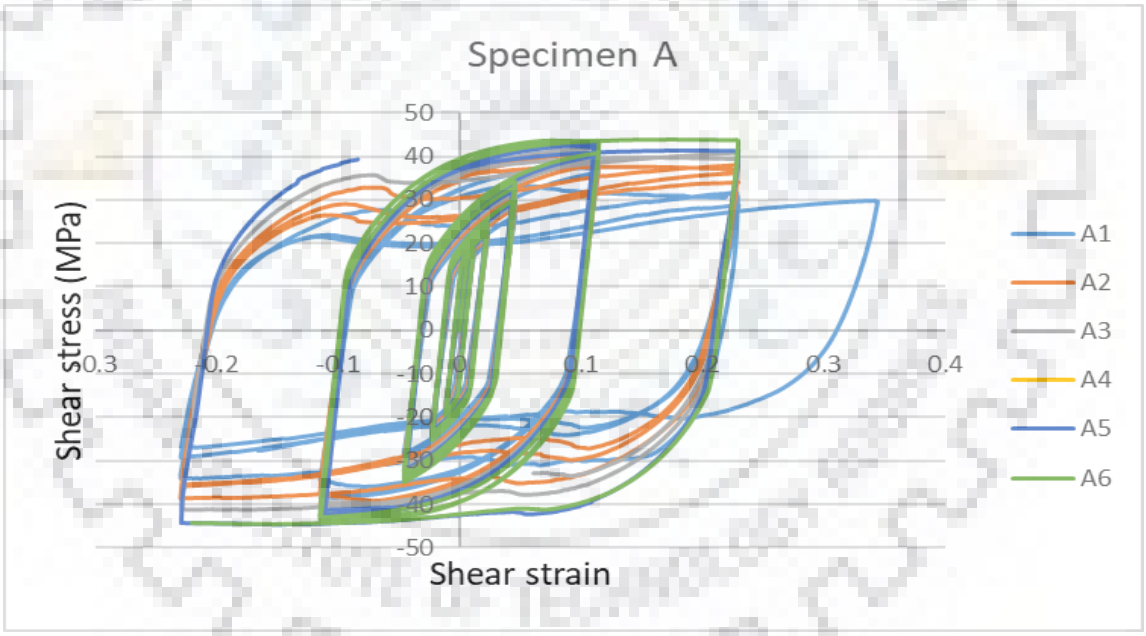

Figure 5.1 Hysteresis curve of the models A1 to A6

Here we can observe that the specimen A1 has shown higher ductile behavior but could resist lesser stress values as compared to remaining 5 models.

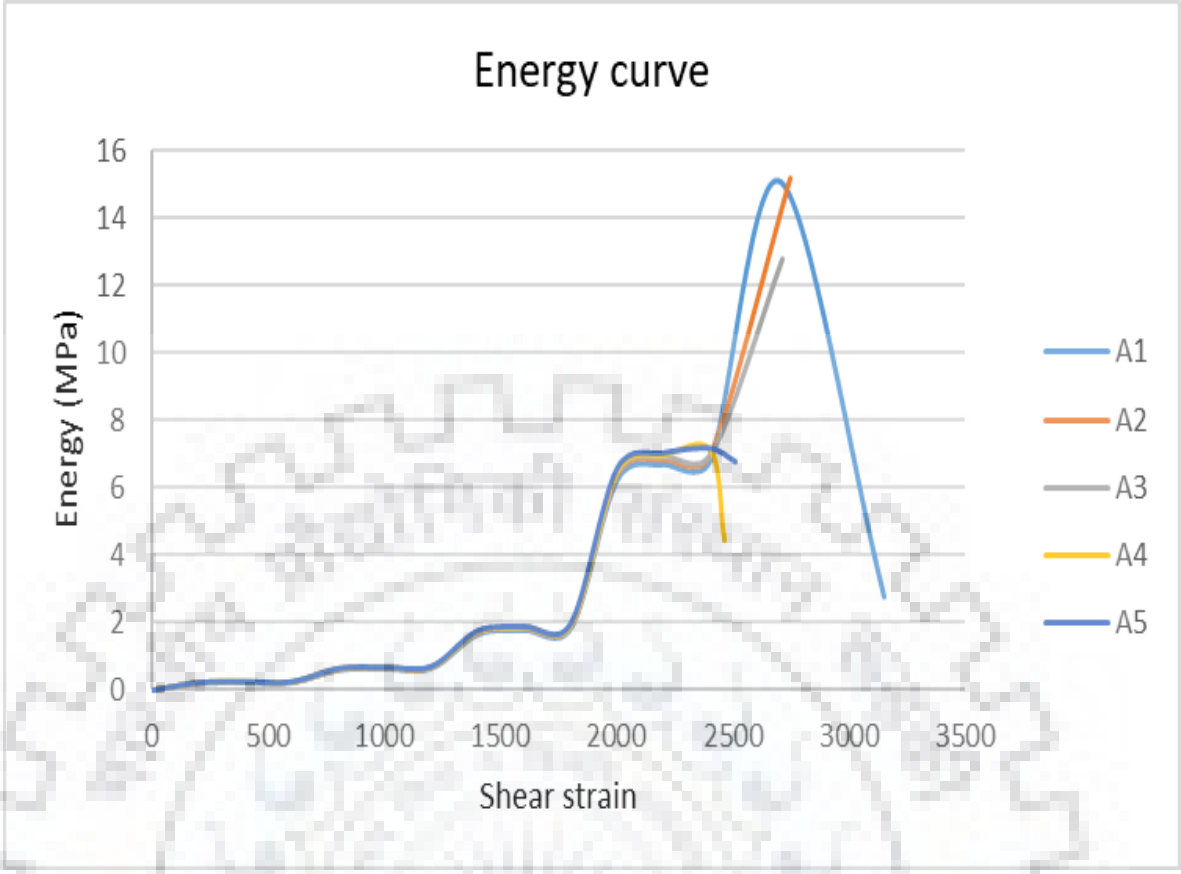

Figure 5.2 Energy curves generated and calculated from hysteresis plots.

Here we can observe that the specimen A1 has shown higher ductile behaviour with comparison to other models in terms of energy dissipation and increment which indirectly defines the strain cycles, but could resist lesser stress values as compared to remaining 5 models. A6 has shown a higher stress value but on the contrary it has shown a faster and lesser energy dissipation and no of cycles it has restrained on higher strain rate is less.

Here we have continuously increased the length of the web, with which the depending value that is the alpha α value has increased from .5 to 2. With which the behaviour has not varied a much but, for other models B1 to K6 there has been a significant difference in the behaviour as the length of the web increases there are many internal failures and a large area of material is not used and failed early.

5.2 Observation of the behavior of damper when we vary only β

Table 5.3 Showing the different dimensions used to generate the models A1, D1, F1, H1

	b_f mm	d_w mm	C mm	α	t_w mm	β	t_s mm
A1	100	350	175	0.5	10	35	20
D1	100	350	175	0.5	5	70	10
F1	100	350	175	0.5	35	10	70
H1	100	350	175	0.5	17.5	20	35

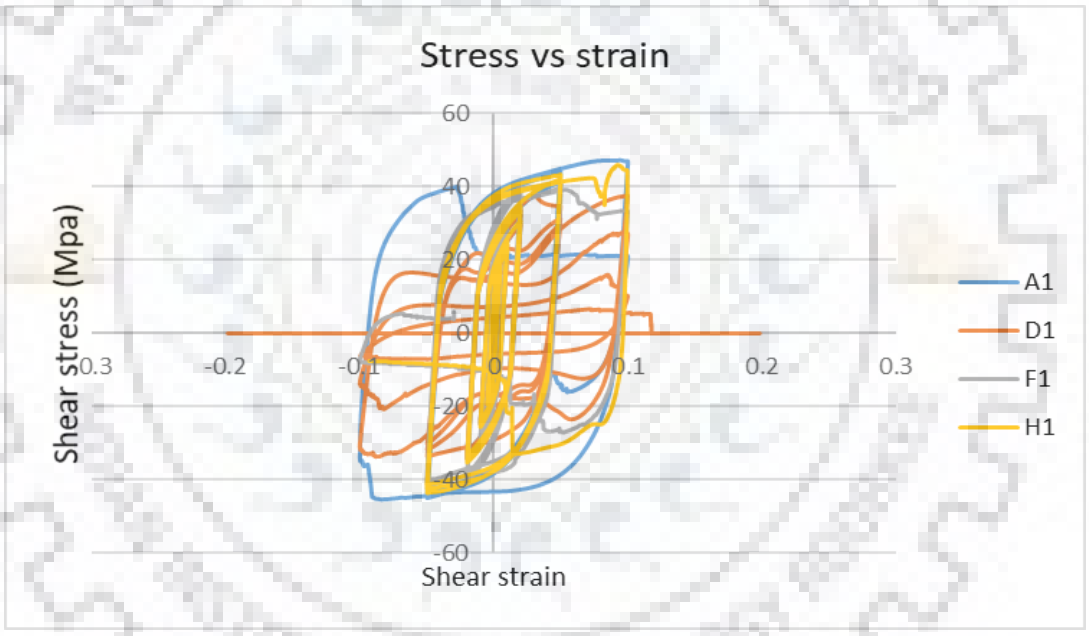

Figure 5.3 Hysteresis curves shear stress (MPa) vs shear strain of the models with same α value but different β

All the remaining factors that effect the behaviour of the damper are kept same varying the thickness of the web that dominantly takes the shear. From the above hysteresis curves we can interpret that the specimen A is showing comparatively better behaviour that the remaining samples in terms of ductility till .15 shear strain. Since D model is having the least web thickness and stiffener thickness the shear stress resisting capacity is less and fails with high ductile cycle with less load carrying capacity.

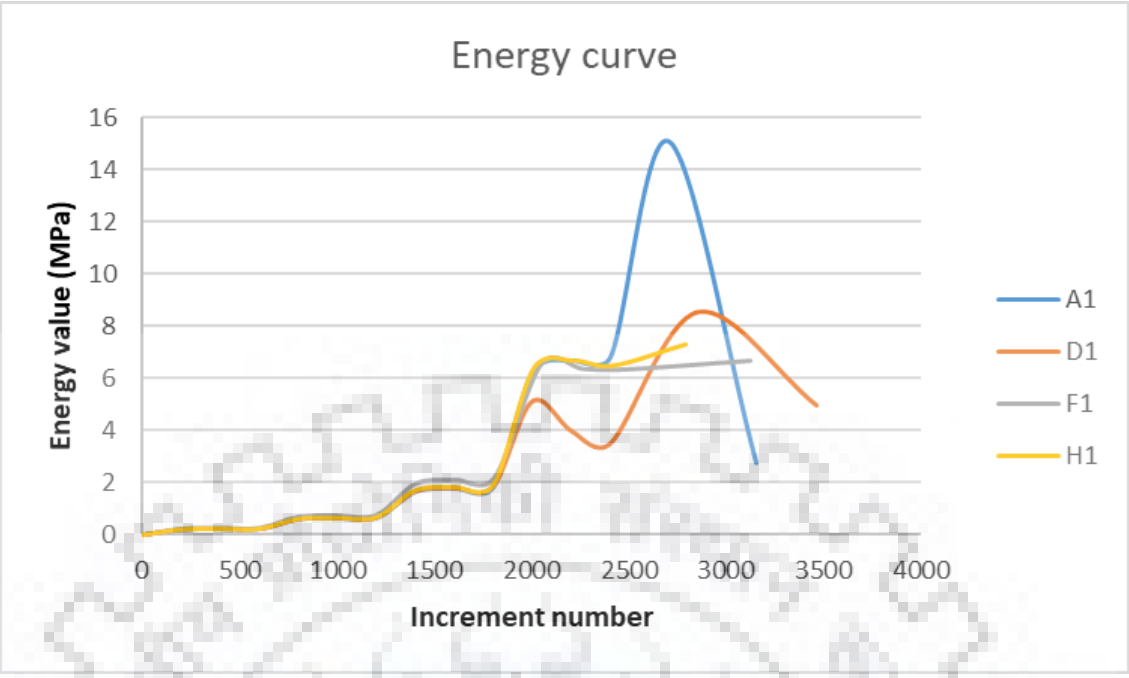

Figure 5.4 Energy curve plotting the energy value vs increment number.

Here we can see that the specimen A1, D1 with lesser thickness of web showed a inelastic range but the remaining specimens didn't show inelastic buckling range due to convergence issues due to large deformations or stress variations.

5.3 Observation of the behavior of damper when we vary only number of panels

Table 5.4 Dimension used to generate the model A1, B1, C1

	b_f mm	d_w mm	C mm	α	t_w mm	β	t_s mm	Panel number
A1	100	350	175	0.5	10	35	20	1
B1	100	350	175	0.5	10	35	20	2
C1	100	350	175	0.5	10	35	20	3

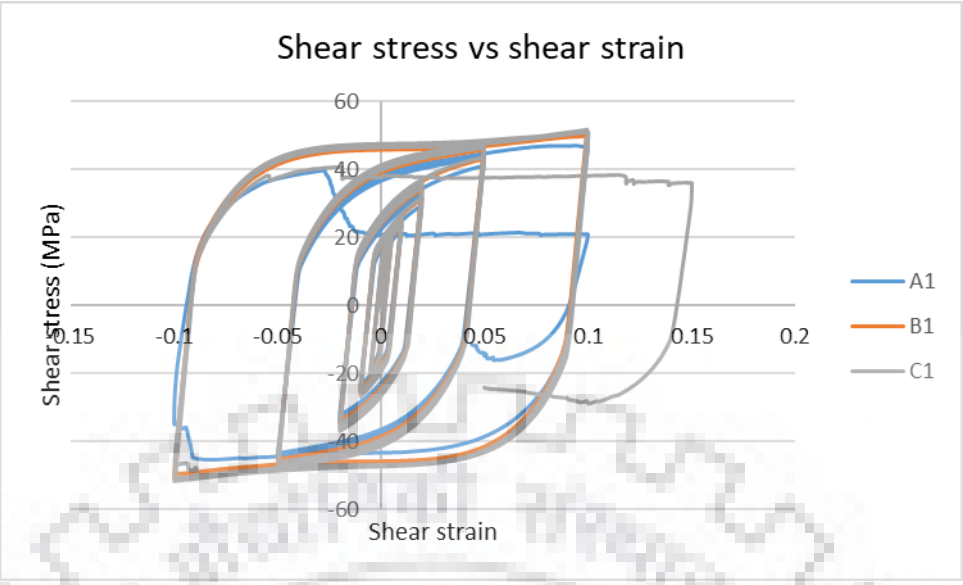

Figure 5.5 Hysteresis curve plotting shear stress (MPa) vs shear strain variation with respect to number of panels

From the above graph we can interpret that number of panels shows a considerable difference in the energy dissipation capacity of the dampers.

The model with 3 panels has shown a considerably better behaviour as compared to model B which has 2 panels. Model A has shown sudden deterioration of the stress values in the final cycle due to the absence of the intermediate stiffener. Due to end stiffeners have to resist the panel buckling due to compressive force created by the action of shear on the damper.

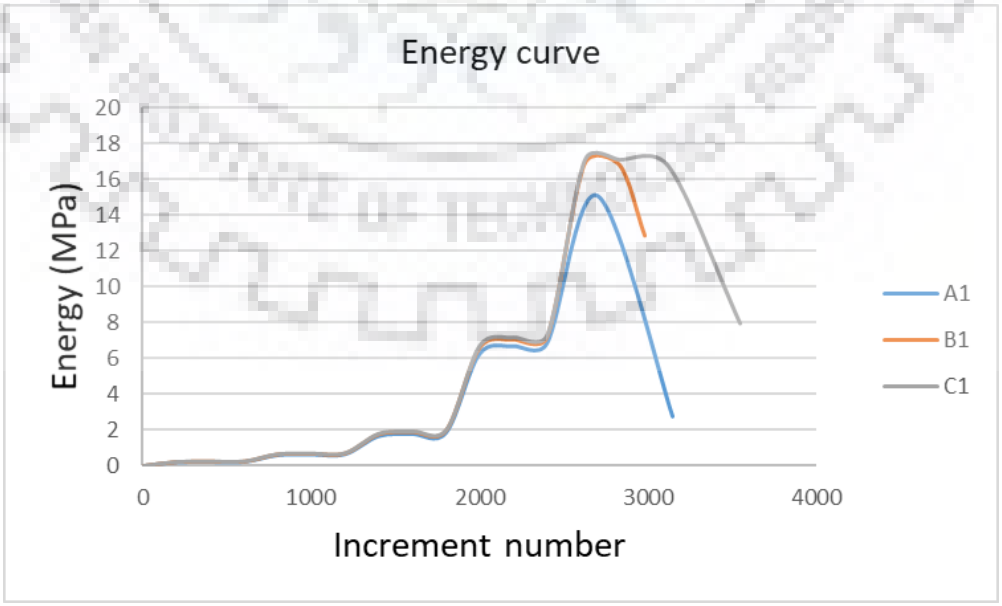

Figure 5.6 Energy curve in MPa with respect to increment value of A1, B1, C1

We can clearly observe the difference in the behavior of damper wrt to number of panel keeping all the other parameters same. The specimen C1 has shown a better behavior wrt to the number of increments and the energy dissipation value as compared to a single panel damper A1. And also we can observe that after the inelastic buckling has taken place the residual strength or energy dissipation capacity of the B1 and C1 are superior and stable due to the available stiffeners. Indeed C1 showed a stable deterioration after the inelastic buckling has taken place.

5.4 Variation of web thickness keeping remaining all factors same

Table 5.5 keeping remaining all factors same and only varying the web thickness in 2 web panels

Name	b_f mm	d_w mm	C mm	α	C mm	t_w mm	β	Thickness Of end stiffener
I1	100	350	380	0.5	175	5	70	10
J1	100	350	500	0.5	175	25	14	50
K1	100	350	560	0.5	175	35	10	70
L1	100	350	434	0.5	175	14	25	28
M1	100	350	455	0.5	175	17.5	20	35

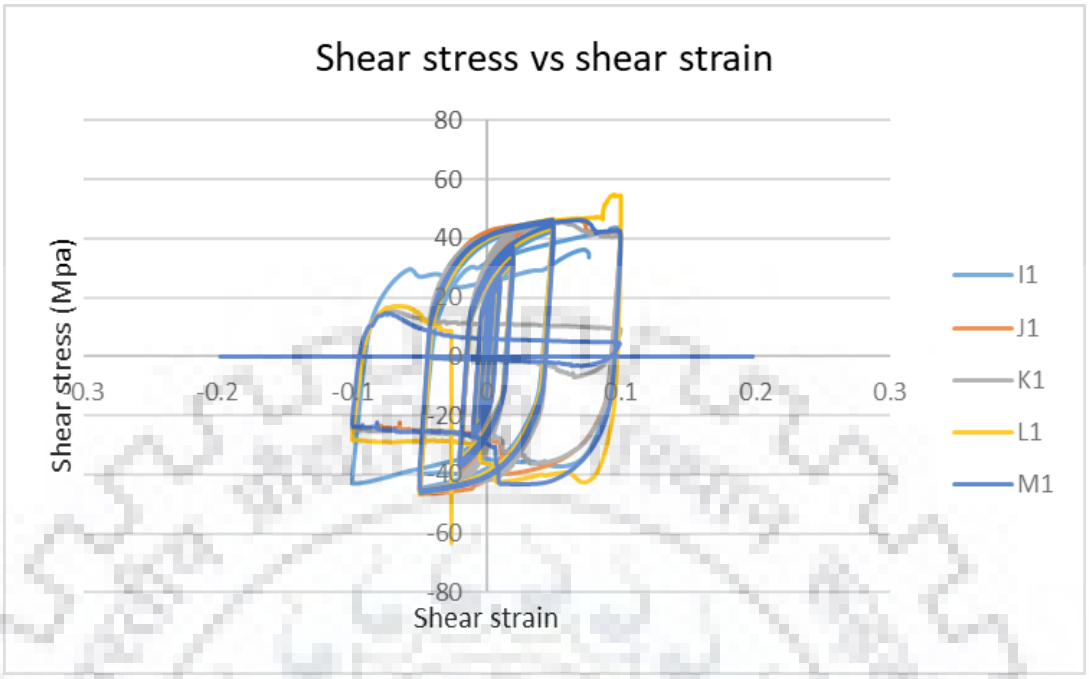

Figure 5.7 Hysteresis curve i.e. shear stress (MPa) variation with respect to thickness of web in damper with 2 panels

From the following curves we can observe that there is a lot of change in the dimension with respect to the thickness of the web, but contradiction to that there is less increase in the superiority in the behavior of the dampers in terms of shear stress and strain values which depicts a conclusion which suggest beyond a point the thickness of web alone doesn't play a major role in increasing the hysteresis behavior of the damper.

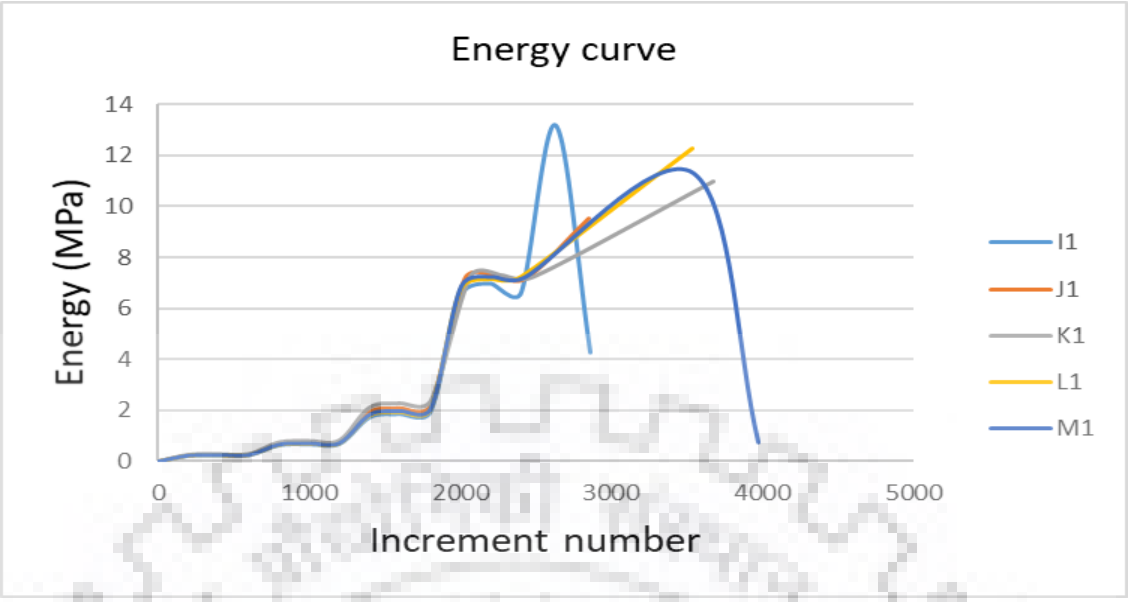

Figure 5.8 Figure showing the energy vs increment number variation of I1, J1, K1, L1, M1.

But the energy curves obtained by the area calculation of the hysteresis curves vs the increment number at which it is obtained show that the specimen M1 and K1 shown a better behavior wrt the no of increments which indirectly implies the no of cycles.

But on the other hand the specimen I1 and L1 have shown a better behavior wrt to energy which implies they have withstanded a larger stress values as compared to M1.

The following table consist of the dimensions adopted in the parametric study of the shear dampers with α variation from A1 to A6 keeping all the remaining factors same and number of panels considered as one.

In B we have considered a variation in the number of panels which is taken as two.and internally in B from B1 to B6 there is again a variation of α mainly the length of the panel or in other words the clear spacing between stiffeners. Similarly in C we have considered the panel to be 3 and internally from C1 to C6 the variation is in the α.

Later in D, E, F, G, H, there is a variation in β mainly the web depth is taken constant so the variation is only in the thickness of web with which the thickness of the stiffeners is also varied by considering the web thickness to stiffener thickness ratio. As we know the thickness of the internal stiffener for the single panel system is obviously zero. In the following study we have taken mostly the thickness of flange to be twice that of the thickness of the web but the variation due to the thickness of the flange is not a good

amount so it doesn't incur a much difference in the overall result of the model to show that there are specimens S, T varying the flange thickness keeping all the other factors same across single panel system and double panel system since there is no variation observed the triple panel specimens are skipped to minimize the time loss.

5.5 Variation of flange thickness keeping remaining all factors same

Figure 5.9 Hysteresis plot between specimen S1, S3, S4, S5

As we can observe there is no much diference due to change in flange thickness so we adopted 0.5 as the ratio of thickness through out the study.

Table 5.6 Variation in the thickness of flange

	width of flange	thickness of web	beta	thick. of end stiffener	thick. of intermediate stiffener	thickness of flange	no. of panels	t_w/t_s	t_w/t_f	t_{es}/t_{is}
S1	100	17.5	20	17.5	17.5	17.5	1	1	1	1
S2	100	17.5	20	17.5	17.5	35	1	1	0.5	1
S3	100	17.5	20	17.5	17.5	23.33	1	1	0.75	1
S4	100	17.5	20	17.5	17.5	70	1	1	0.25	1
S5	100	17.5	0	17.5	17.5	140	1	1	0.125	1

6 DESIGN OF ALUMINIUM DAMPER BASED ON THE ANALYTICAL RESULTS

Design of specimen A1 is shown and the same process is followed through all the specimens. All the values used for calculations are tabulated in table 6.1. The results of the calculations are shown in table 7.1. the input for these calculations are obtained from Abaqus modelling results that are plotted in appendix-1 i.e. the shear stress vs shear strain plots the energy curves and backbone curves.

Young's modulus of the model E=16.88*10^9 Pa

Buckling coefficient of the specimen A1 $K_s = 8.98 + \frac{5.6}{\alpha^2}, for(\alpha > 1)$ (7.1)

$$K_s = 5.6 + \frac{8.98}{\alpha^2}, for(\alpha \leq 1) \quad (7.2)$$

For A1 $\alpha = .5$

So we must use the following equation for calculating the buckling coefficient of the specimen, $K_s = 5.6 + \frac{8.98}{\alpha^2}, for(\alpha \leq 1)$

K_s=41.52

Elastic buckling stress of the specimen A1, $\tau_e = K_s \pi^2 E \frac{1}{12(1-\mu^2)}\left(\frac{1}{\beta^2}\right)$ (7.3)

The ratio of depth of the web to the thickness of the web, $\beta = 35$

$\tau_e = 528MPa$

The slenderness ratio of the panel as per aluminium association,

$$\lambda = \alpha \times \beta \times \sqrt{\frac{1.2}{1+0.63\alpha^2}} \text{ for } \alpha < 1 \quad (7.4)$$

$$\lambda = \beta \times \sqrt{\frac{1.2}{1+\frac{0.63}{\alpha^2}}} \text{ for } \alpha > 1 \quad (7.5)$$

λ =17.81

The inelastic buckling stress of the specimen A1, $\tau_b = \frac{\pi^2 Et}{\lambda^2}$ (7.6)

E_t is tangential Young's modulus of the model which is taken to be 15% of original Young's modulus

Inelastic buckling stress after calculation, τ_b =59.97 MPa

Buckling stress ratio $\frac{\tau_b}{\tau_e} = 0.11368$

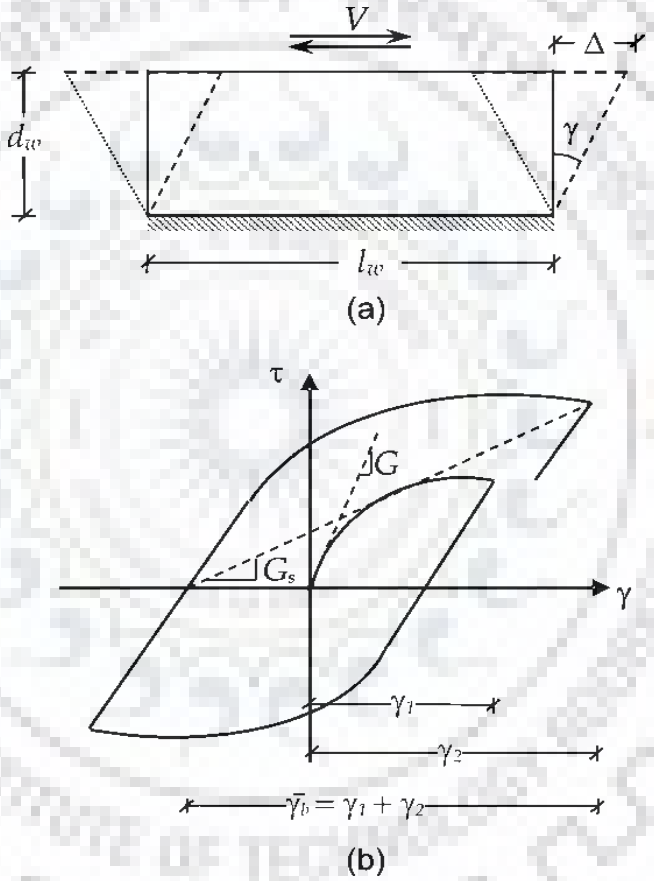

Figure 6.1 (a). Shear deformation of the web panel. (b). Definition of secant shear modulus (G_s) and shear modulus of the specimen (G)

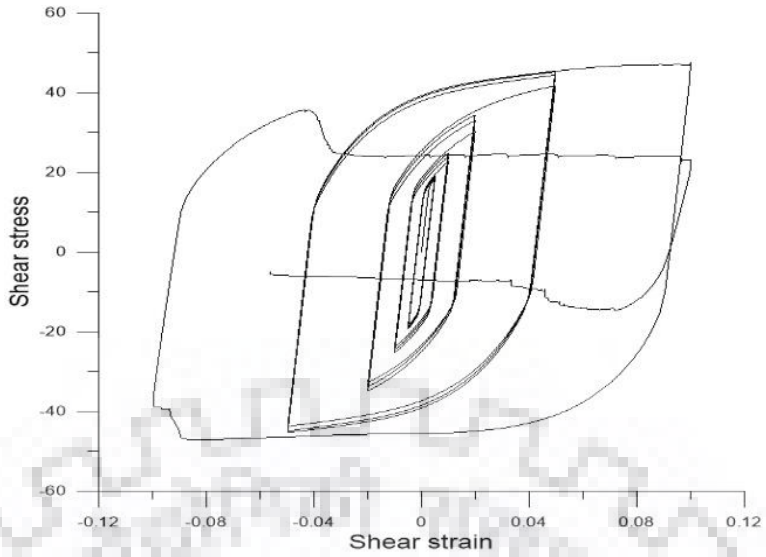

Figure 6.2 Shear stress vs shear strain result obtained from abaqus model analysis

The secant shear modulus of the specimen that is calculated from the Abaqus model results as shown in the above figure G_s= 497.7180632

The shear modulus which has been obtained from the analytical results plot between shear stress and shear strain G= 6166.605684

Shear modulus ratio G_s/G= 0.080711835

F (proportionality factor) as per Gerard's formulation about the shear dampers which is a ratio of inelastic buckling stress ratio to secant shear modulus ratio= $\frac{\frac{\tau_b}{\tau_e}}{\frac{G_s}{G}}$ 1.408549913

The following calculation is a model calculation which is followed for all the specimens from A1 till R4 and their proportionality factor is the main source of interest and the behavior of the sample taken in terms of the backbone curve variation so as to understand the main points of interest i.e. the variation of the stress under different cycles of strain

Table 6.1 Design parameters of the aluminium shear panel generated from Gerard's formulation.

Name	Lamda	K_s	Elastic buckling stress	Inelastic buckling stress	Inelastic/Elastic	Shear modulus	Secant shear modulus	Secant modulus/ Shear modulus	F Proportionality factor
A1	17.82	41.52	527.53	78.77	0.15	5462.46	475.86	0.09	1.71
A2	24.71	21.56	273.98	40.96	0.15	5839.95	229.66	0.04	3.80
A3	30.03	14.58	185.24	27.73	0.15	6046.07	242.33	0.04	3.74
A4	32.37	12.56	159.63	23.87	0.15	6173.99	420.56	0.07	2.20
A5	33.89	11.47	145.72	21.78	0.15	6261.86	411.02	0.07	2.28
A6	35.64	10.38	131.88	19.69	0.15	6374.37	455.25	0.07	2.09
B1	17.82	41.52	527.53	78.77	0.15	6166.61	497.72	0.08	1.85
B2	24.71	21.56	273.98	40.96	0.15	6343.21	480.35	0.08	1.97
B3	30.03	14.58	185.24	27.73	0.15	6435.69	109.77	0.02	8.78
B4	32.37	12.56	159.63	23.87	0.15	6493.04	459.30	0.07	2.11
B5	33.89	11.47	145.72	21.78	0.15	6531.22	455.72	0.07	2.14
B6	35.64	10.38	131.88	19.69	0.15	6580.41	447.35	0.07	2.20
C1	17.82	41.52	527.53	78.77	0.15	6416.63	485.12	0.08	1.98
C2	24.71	21.56	273.98	40.96	0.15	6519.86	467.28	0.07	2.09
C3	30.03	14.58	185.24	27.73	0.15	6572.36	459.82	0.07	2.14
C4	32.37	12.56	159.63	23.87	0.15	6604.18	458.49	0.07	2.15
C5	33.89	11.47	145.72	21.78	0.15	6624.79	458.80	0.07	2.16
C6	35.64	10.38	131.88	19.69	0.15	6652.18	469.10	0.07	2.12
D1	35.64	41.52	131.88	19.69	0.15	5567.26	334.82	0.06	2.48
D2	49.42	21.56	68.50	10.24	0.15	5179.66	439.57	0.08	1.76
D3	60.06	14.58	46.31	6.93	0.15	5777.39	308.46	0.05	2.80
D4	64.73	12.56	39.91	5.97	0.15	5905.20	321.21	0.05	2.75

Name	Lamda	K_s	Elastic buckling stress	Inelastic buckling stress	Inelastic/Elastic	Shear modulus	Secant shear modulus	Secant modulus/ Shear modulus	F Proportionality factor
D5	67.78	11.47	36.43	5.44	0.15	5992.90	336.18	0.06	2.66
D6	71.27	10.38	32.97	4.92	0.15	6102.84	297.26	0.05	3.07
E1	7.13	41.52	3297.05	492.33	0.15	5601.32	426.35	0.08	1.96
E2	9.88	21.56	1712.40	256.03	0.15	5933.30	438.74	0.07	2.02
E3	12.01	14.58	1157.78	173.33	0.15	6124.76	445.58	0.07	2.06
E4	12.95	12.56	997.69	149.21	0.15	6246.83	447.66	0.07	2.09
E5	13.56	11.47	910.73	136.11	0.15	6333.70	400.37	0.06	2.36
E6	14.25	10.38	824.26	123.08	0.15	6448.16	424.90	0.07	2.27
F1	5.09	41.52	6462.21	964.97	0.15	7070.56	428.20	0.06	2.47
F2	7.06	21.56	3356.31	501.82	0.15	7297.12	442.01	0.06	2.47
F3	8.58	14.58	2269.25	339.72	0.15	7428.11	442.66	0.06	2.51
F4	9.25	12.56	1955.47	292.45	0.15	7515.18	457.36	0.06	2.46
F5	9.68	11.47	1785.03	266.77	0.15	7575.92	467.29	0.06	2.42
F6	10.18	10.38	1615.55	241.24	0.15	7657.27	442.89	0.06	2.58
G4	23.12	12.56	312.88	46.79	0.15	6334.90	416.10	0.07	2.28
G5	24.21	11.47	285.60	42.68	0.15	6421.56	457.82	0.07	2.10
G6	25.45	10.38	258.49	38.60	0.15	6533.02	458.61	0.07	2.13
H1	10.18	41.52	1615.55	241.24	0.15	5829.76	441.09	0.08	1.97
H2	14.12	21.56	839.08	125.46	0.15	6174.40	449.07	0.07	2.06
H3	17.16	14.58	567.31	84.93	0.15	6366.60	453.45	0.07	2.10
H4	18.50	12.56	488.87	73.11	0.15	6489.58	484.88	0.07	2.00
1H4	18.50	12.56	488.87	73.11	0.15				
H5	19.36	11.47	446.26	66.69	0.15	6573.19	437.79	0.07	2.24
H6	20.36	10.38	403.89	60.31	0.15	6683.48	452.95	0.07	2.20

Name	Lamda	K_s	Elastic buckling stress	Inelastic buckling stress	Inelastic/Elastic	Shear modulus	Secant shear modulus	Secant modulus/ Shear modulus	F Proportionality factor
I1	35.64	41.52	131.88	19.69	0.15	5924.38	448.55	0.08	1.97
I2	49.42	21.56	68.50	10.24	0.15	6121.12	328.01	0.05	2.79
I3	60.06	14.58	46.31	6.93	0.15	6223.84	327.19	0.05	2.85
I4	64.73	12.56	39.91	5.97	0.15	6284.41	309.85	0.05	3.03
I5	67.78	11.47	36.43	5.44	0.15	6326.38	366.78	0.06	2.58
I6	71.27	10.38	32.97	4.92	0.15	6377.91	365.37	0.06	2.61
J1	7.13	41.52	3297.05	492.33	0.15	7103.96	488.24	0.07	2.17
J2	9.88	21.56	1712.40	256.03	0.15	7199.38	435.15	0.06	2.47
J3	12.01	14.58	1157.78	173.33	0.15	7249.58	488.84	0.07	2.22
J4	12.95	12.56	997.69	149.21	0.15	7278.42	489.96	0.07	2.22
J5	13.56	11.47	910.73	136.11	0.15	7298.57	457.31	0.06	2.39
J6	14.25	10.38	824.26	123.08	0.15	7326.95	436.95	0.06	2.50
K1	5.09	41.52	6462.21	964.97	0.15	7929.66	478.83	0.06	2.47
K2	7.06	21.56	3356.31	501.82	0.15	7956.29	492.34	0.06	2.42
K3	8.58	14.58	2269.25	339.72	0.15	7962.36	985.59	0.12	1.21
K4	9.25	12.56	1955.47	292.45	0.15	7964.11	491.45	0.06	2.42
K5	9.68	11.47	1785.03	266.77	0.15	7964.06	1034.49	0.13	1.15
K6	10.18	10.38	1615.55	241.24	0.15	7962.72	466.18	0.06	2.55
L1	12.73	41.52	1033.95	154.39	0.15	6386.52	488.74	0.08	1.95
L2	17.65	21.56	537.01	80.29	0.15	6542.49	468.52	0.07	2.09
L3	21.45	14.58	363.08	54.35	0.15	6626.89	414.98	0.06	2.39
L4	23.12	12.56	312.88	46.79	0.15	6677.29	483.00	0.07	2.07
L5	24.21	11.47	285.60	42.68	0.15	7938.90	547.28	0.07	2.17
L6	25.45	10.38	258.49	38.60	0.15	6759.79	443.55	0.07	2.28

Name	Lamda	K_s	Elastic buckling stress	Inelastic buckling stress	Inelastic/Elastic	Shear modulus	Secant shear modulus	Secant modulus/ Shear modulus	F Proportionality factor
M1	10.18	41.52	1615.55	241.24	0.15	6593.36	480.70	0.07	2.05
M2	14.12	21.56	839.08	125.46	0.15	6738.09	410.36	0.06	2.46
M3	17.16	14.58	567.31	84.93	0.15	8702.26	539.68	0.06	2.41
M4	18.50	12.56	488.87	73.11	0.15				
M5	19.36	11.47	446.26	66.69	0.15				
M6	20.36	10.38	403.89	60.31	0.15				
N1	35.64	41.52	131.88	19.69	0.15	6151.74	454.92	0.07	2.02
N2	49.42	21.56	68.50	10.24	0.15	6153.98	446.79	0.07	2.06
N3	60.06	14.58	46.31	6.93	0.15	6341.12	456.11	0.07	2.08
N4	64.73	12.56	39.91	5.97	0.15	6153.10	441.76	0.07	2.08
O1	7.13	41.52	3297.05	492.33	0.15	6153.10	441.76	0.07	2.08
O2	9.88	21.56	1712.40	256.03	0.15	7423.89	479.97	0.06	2.31
O3	12.01	14.58	1157.78	173.33	0.15	7424.80	466.03	0.06	2.39
O4	12.95	12.56	997.69	149.21	0.15	7424.86	454.82	0.06	2.44
P1	5.09	41.52	6462.21	964.97	0.15	8265.62	467.71	0.06	2.64
P2	7.06	21.56	3356.31	501.82	0.15	8204.02	484.28	0.06	2.53
P3	8.58	14.58	2269.25	339.72	0.15	8161.03	457.20	0.06	2.67
P4	9.25	12.56	1955.47	292.45	0.15	8126.03	466.41	0.06	2.61
Q1	12.73	41.52	1033.95	154.39	0.15	6649.69	427.59	0.06	2.32
Q2	17.65	21.56	537.01	80.29	0.15	6733.89	466.18	0.07	2.16
Q3	21.45	14.58	363.08	54.35	0.15	6772.68	457.77	0.07	2.21
Q4	23.12	12.56	312.88	46.79	0.15	6800.74	448.74	0.07	2.27
R1	10.18	41.52	1615.55	241.24	0.15	6872.01	456.83	0.07	2.25
R2	14.12	21.56	839.08	125.46	0.15	6932.99	431.02	0.06	2.40

Name	Lamda	K_s	Elastic buckling stress	Inelastic buckling stress	Inelastic/Elastic	Shear modulus	Secant shear modulus	Secant modulus/ Shear modulus	F Proportionality factor
R3	17.16	14.58	567.31	84.93	0.15	6970.56	461.84	0.07	2.26
R4	18.50	12.56	488.87	73.11	0.15	6982.37	451.97	0.06	2.31

7 OBSERVATION OF THE FACTORS AFFECTING THE DESIGN CONSIDERATIONS

7.1 Tension field action

The strength of aluminium plate members is generally controlled by buckling. The factors that affect the buckling of aluminium plates are configuration/shape of the plate, type of loading, fixity of the edges, alloy and temper etc. In case of plate girder, they are designed in such a way that eve after buckling they can carry load with a phenomenon called tension field action. When the girder is loaded beyond its limit first it will deflect significantly because it has lost its stiffness, but after significant defection, the profile of girder will be too curved so the web in the region between the stiffeners will experience tension which will be directed towards the support. This will cause some truss kind of action with the stiffeners as vertical members of truss, compression flange as top chord, tension flange as tie member and our web as diagonal member. Now this girder will again carry a good amount of load just because of this action. This is tension field action of plate girder where the web plays an important role.

7.2 End stiffeners

The tension field in the shear panel is resisted by the flanges and by the adjacent panels and transverse stiffeners. Since the panels adjacent to an interior panel in a specimen having three panels is able to resist tension field. They can be counted on to furnish the necessary support. However, an end panel does not have such support thus end stiffeners undergo large bending while resisting the bending effects of tributary tension field. In almost all the specimens, end stiffener bent much more and at lower strain levels as compared to intermediate transverse stiffeners. The end stiffeners help in control of the amplitude of web buckling and thereby reduce the severity of resistance capacity deterioration of the panel upon cycling. The end stiffeners appeared to be much more bent due to tension field, while intermediate transverse stiffeners do not show much bending. The analytical predictions are compared with the results of available experimental test results, showing good agreement.

7.3 Effect of aspect ratio,

The function of transverse stiffener is to subdivide the panel web into smaller panels, thereby increasing the shear buckling stress. The effect of providing stiffener is to delay

the onset of web buckling. Delaying the web buckling allowed the web to continue to strain harden and permitted the specimen to reach the peak stress. The web of the aluminum section was reinforced with transverse stiffeners to increase its resistance to buckling. Hence, reduction in the spacing of transverse stiffeners results into the lower value of aspect ratio, of the panel thus resulting in increase in web buckling deformation angle.

7.4 Effect of web depth-to-thickness ratio,

For the web depth-to-thickness ratio 20-35, certain specimen showed no buckling at all, even at strains upto 0.20 or sometimes even completely avoiding web buckling until the tearing of web plate. But some specimens with web depth to thickness ratio greater than 35 failed at 0.1 strain values. Thus, as web depth-to-thickness ratio is increased, the tendency of buckling of the panel is delayed to larger strain levels.

7.5 Effect of number of panels

It is evident that in model with 3 panels has shown a considerably better behaviour as compared to model B which has 2 panels in terms of shear strain. Thus, it can be stated that three paneled specimen buckled at large strain level as compared to two paneled specimens with other parameters remaining the same.

It can be observed that the ultimate load level achieved in three paneled specimens is slightly larger than 1.5 times the corresponding two paneled specimens with other parameters as same. This may be due to the tension field developed in the central panel is resisted by the adjacent outer panel web which is not in case of two-paneled specimens.

Symbols used in the above report

B_s, D_s- material parameters defined by Aluminium Association

t_w - thickness of web

b- longer dimension of panel

n- number of panels

C- clear spacing of stiffeners

d_w- clear depth of web

E_t- tangent modulus

f- constant as defined in Gerard's formulation

G- shear modulus

G_s- shear secant modulus

0.2- proof stress corresponding to 0.2% strain

k_s- buckling coefficient

l_w- length of web

E- Young's modulus

t_s- thickness of stiffeners

V- lateral load

$\frac{8.98}{\alpha^2}$ -ratio of stiffener spacing to clear depth of web

a- shorter dimension of panel

β - web depth-to-thickness ratio

η- plastic-reduction factor

τ - shear stress

γ - elastic shear strain

γ_b - inelastic cyclic shear strain at buckling in Gerard's buckling criterion

λ- Characteristic slenderness ratio

τ_b - inelastic buckling stress

τ_e - elastic buckling stress

τ_y - yield shear stress

REFERENCES

1. Abaqus/CAE *2016* [Computer software]. Dassault Systemes Simulia Corp., Johnston, RI, USA.
2. Aluminum Association, (2005). "Specifications for Aluminum Structures", 5th edition, Aluminum Design Manual, Washington, DC. I-B-24-I-B-40
3. Azhari, M. and Bradford, M. A., (1993). "Inelastic Initial Local Buckling of Plates With and Without Residual Stresses", *Engineering Structures*, 15(1), 31–39.
4. Chen, Z.Y., Bian, G.Q. and Huang, Y. (2011). "Review on Web Buckling and Hysteretic Behavior of Shear Panel Dampers", *International Journal of Advanced Steel Construction*, 9(3), 205–217.
5. Clark, J. W. and Rolf, R. L. (1966). "Buckling of Aluminum Columns, Plates and Beams", *Journal of the Structural Division*, 92(3), 17–38.
6. Constantinou M. C., Soong, T. T. and Dargush, G. F. (1998). "Passive Energy Dissipation Systems for Structural Design and Retrofit", *Monograph No.1. Buffalo (NY): Multidisciplinary Center for Earthquake Engineering Research*, 65-180.
7. Corte, D. G., D'Aniello, M. and Landolfo, R. (2013). "Analytical and Numerical Study of Plastic Overstrength of Shear Links", *Journal of Constructional Steel Research*, 82(1), 19-32.
8. De Matteis, G., Brando, G., Mazzolani, F. M. (2010). "Hysteretic Behaviour of Bracing-type Pure Aluminium Shear Panels by Experimental Tests", *Earthquake Engineering and Structural Dynamics*, 40(10), 1143-1162.
9. De Matteis, G., Landolfo, R. and Mazzolani, F. M. (2003). "Seismic Response of MR Steel Frames with Low-yield Steel Shear Panels", *Engineering Structures – The Journal of Earthquake Wind Ocean Engineering*, 25(1), 155–168.
10. De Matteis, G., Mazzolani, F. M. and Panico, S. (2007). "Pure Aluminium Shear Panels as Dissipative Devices in Moment-resisting Steel Frames", *Earthquake Engineering and Structure Dynamics*, 36, 841–859.

11. Gerard, G. (1948). “Critical Shear Stress of Plates above the Proportional Limit”, *ASME Journal of applied mechanics,* 15(1), 7–12.

12. IS: 2812 (1993), “Recommendations of Manual Tungsten Inert-gas arc Welding of Aluminium and Aluminium alloys”, Bureau of Indian Standards, New Delhi, India.

13. Jain, S., Rai, D. C., Sahoo, D. R. (2008). “**Postyield cyclic buckling criteria for aluminum shear panels**”, *Journal of Applied Mechanics*, 75 (2), 1-8

14. Kasai, K. and Popov, E. P. (1986). “Cyclic Web Buckling Control for Shear Link Beams”, *Journal of Structural Engineering*, 112(3), 505–523.

15. Liu, X. G, Fan, J. S, Liu, Y. F, Yue, Q. R. and Nie, J. G. (2017). “Experimental Research of Replaceable Q345GJ Steel Shear Links Considering Cyclic Buckling and Plastic Overstrength”, *Journal of Constructional Steel Research*, 13(4), 79-160.

16. Manchalwar A. and Bakre S. V. (2016). “Performance of RC Structures Equipped with Steel and Aluminium X-Plate Dampers”, *Journal of Institution of Engineers India,* 97(4), 415-425.

17. *OriginPro 2017* [Computer software]. OriginLab Corporation, Northampton, MA

18. Rai, D. C. (2002). “Inelastic Cyclic Buckling of Aluminium Shear Panels,” *Journal of Engineering Mechanics*, 128(11), 1233–1237.

19. Rai, D. C. and Wallace, B. J. (1998). “Aluminium Shear-Links for Enhanced Seismic Resistance”, *Earthquake Engineering Structure Dynamics*, 27(3), 315–342.

20. Rai, D. C., Annam, P. K. and Pradhan, T. (2004). “Seismic Testing of Steel Braced Frames with Aluminum Shear Yielding Dampers”, *Engineering Structures,* 2012(26), 737–47.

21. Richards, P, Uang, C-. M. (2004). “Development of Testing Protocol for Links in Eccentrically Braced Frames”, *In: Proc. of the 13th World Conference on Earthquake Engineering,* 2-5.

22. Sahoo, D. R., Singhal, T., Taraithia S. and Saini, A. (2015). “Cyclic Behavior of Shear-and-flexural Yielding Metallic Dampers”, *Journal of Constructional Steel Research*, 114, 247–257

23. Yoo, C. H. and Lee, S. C. (2006). “Mechanics of Web Panel Post-Buckling Behaviour in Shear”, *Journal of Structural Engineering*, 132(10), 1580–1589.

24. Zhang, C., Aoki, T., Zhang, Q. and Wu, M. (2015). “The Performance of Low-yield-strength Steel Shear-panel Damper with and without Buckling”, *Materials and Structures*, 48(4), 1233–1242.

APPENDIX-1

Graphs plotted between shear stress (MPa) vs shear strain of specimen A1 to L6

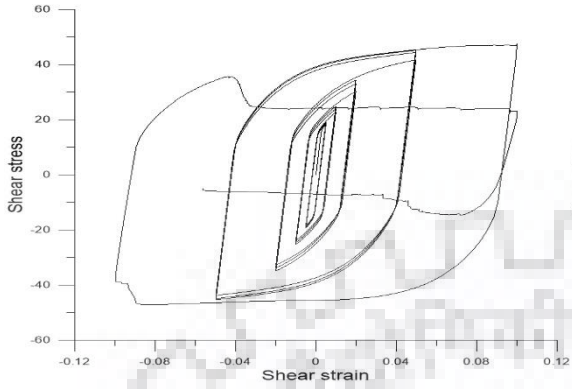

Specimen A1

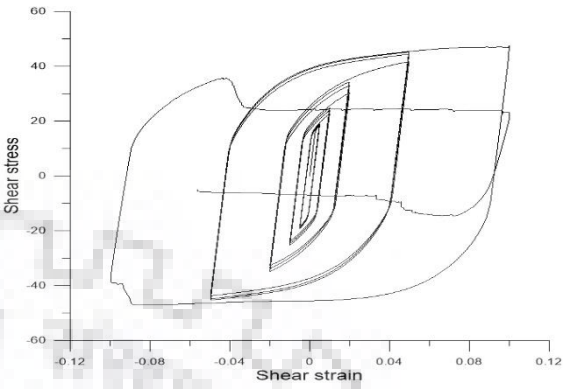

Specimen A2

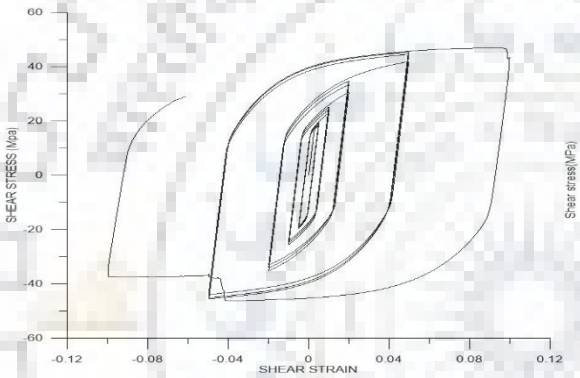

Specimen A3

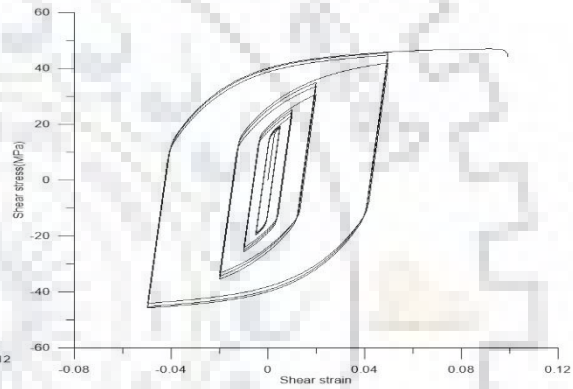

Specimen A4

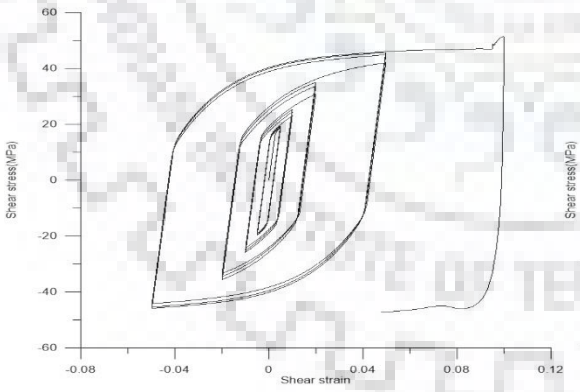

Specimen A5

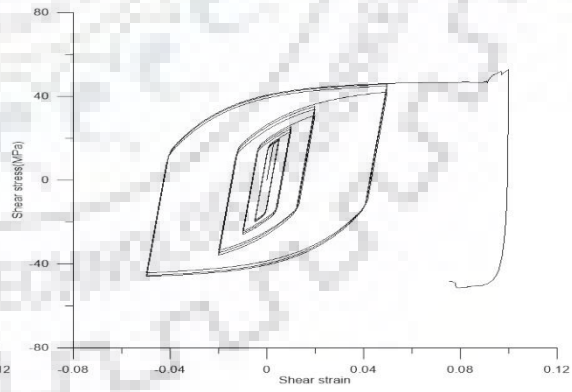

Specimen A6

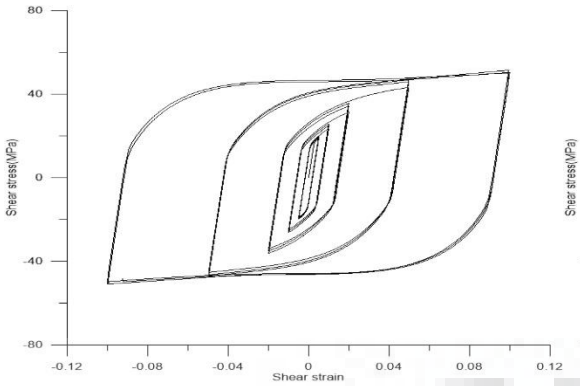

Specimen B1

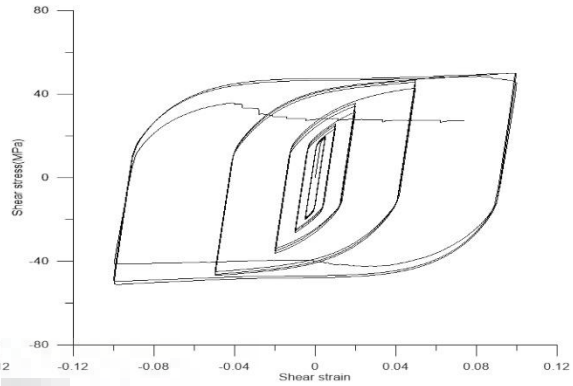

Specimen B2

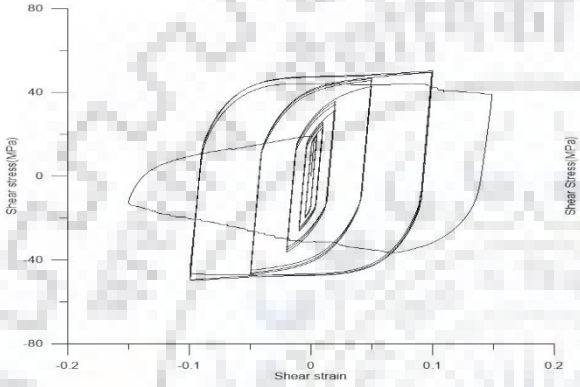

Specimen B3

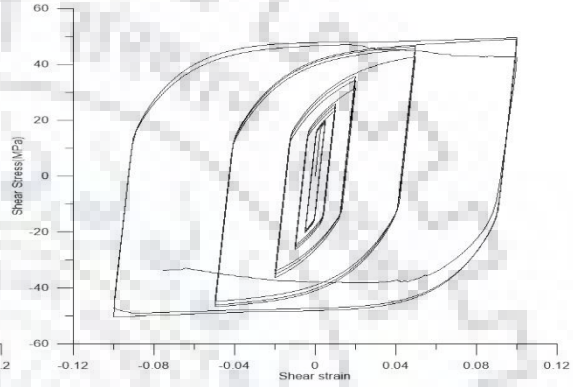

Specimen B4

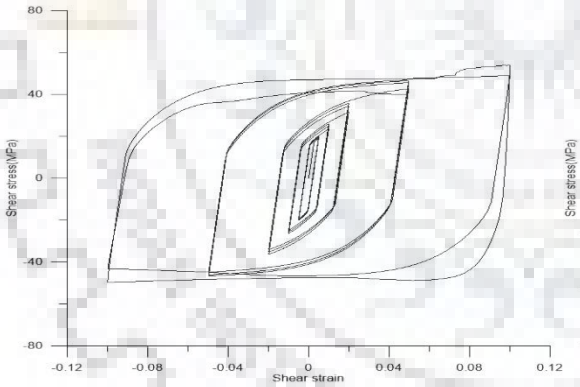

Specimen B5

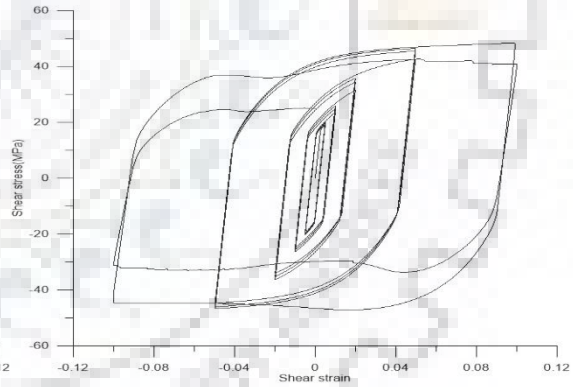

Specimen B6

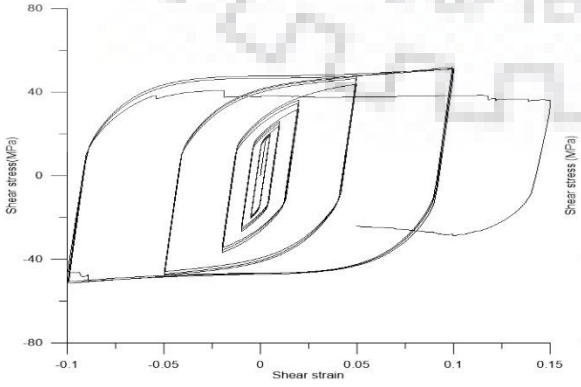

Specimen C1

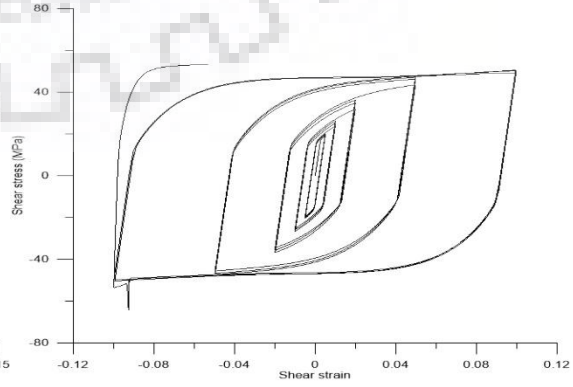

Specimen C2

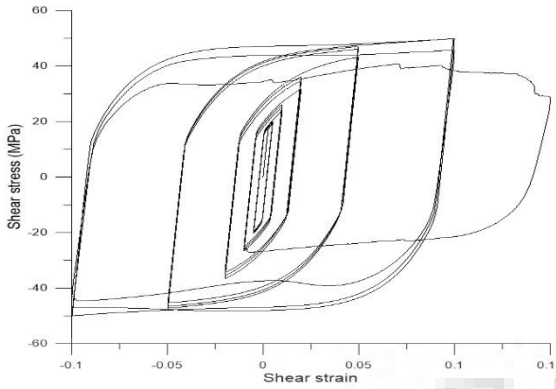

Specimen C3

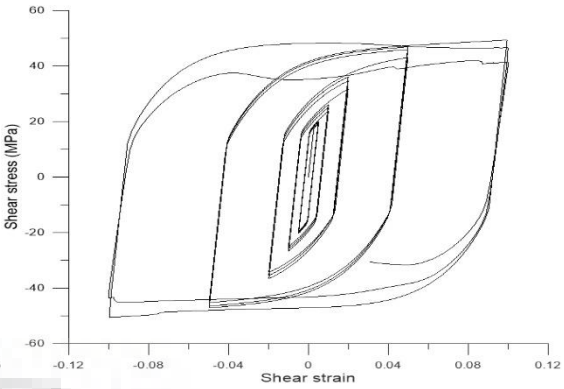

Specimen C4

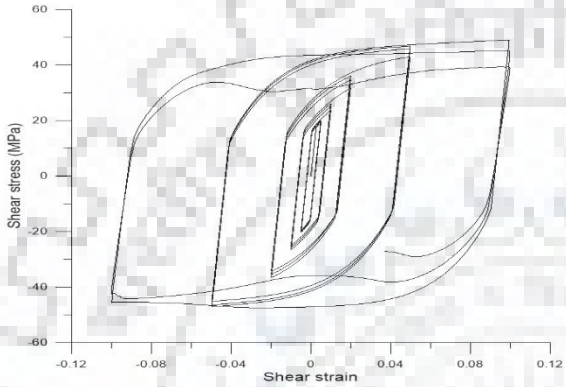

Specimen C5

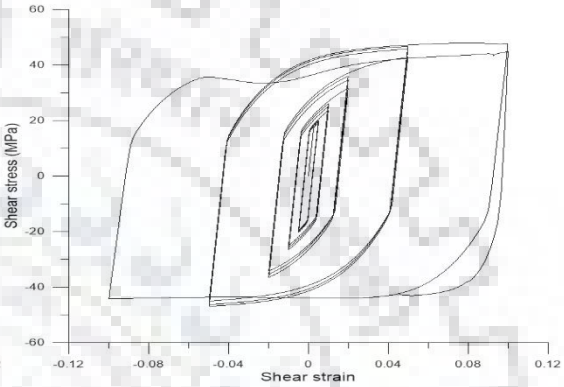

Specimen C6

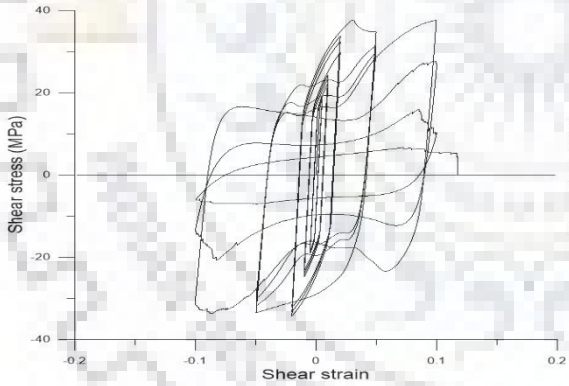

Specimen D1

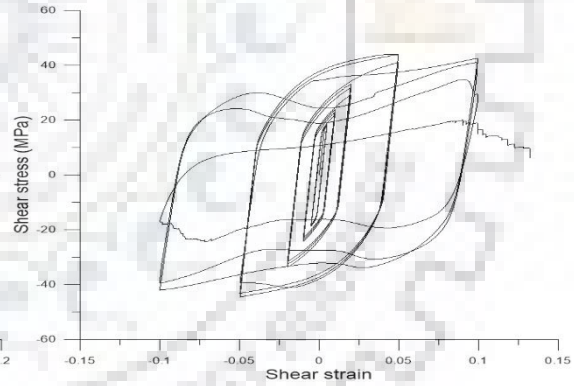

Specimen D2

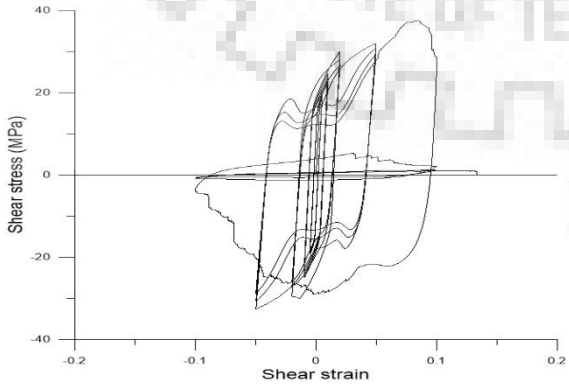

Specimen D3

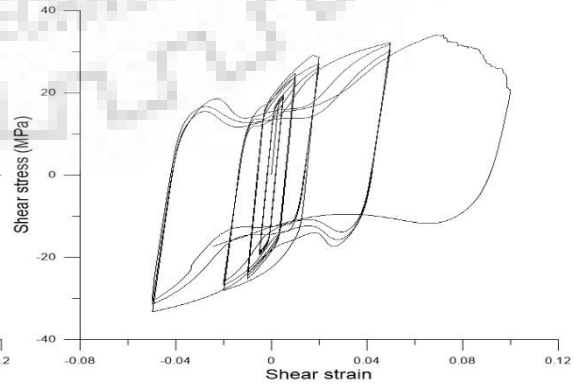

Specimen D4

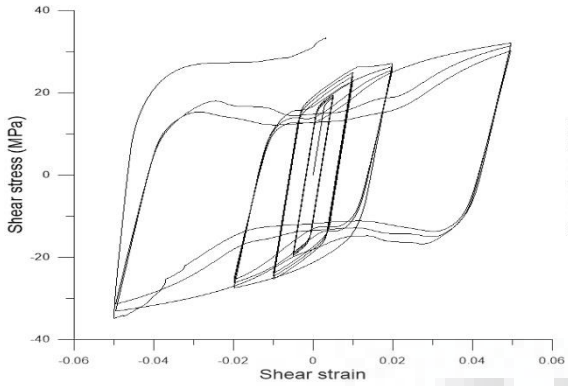

Specimen D5

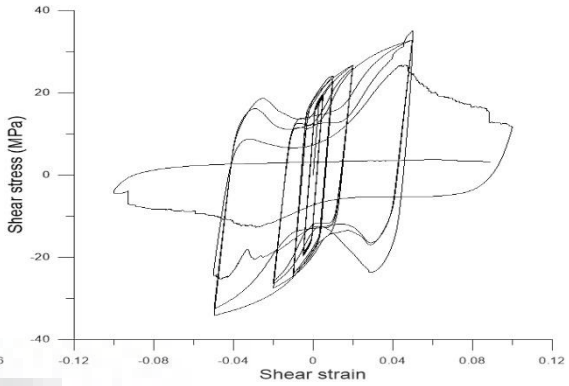

Specimen D6

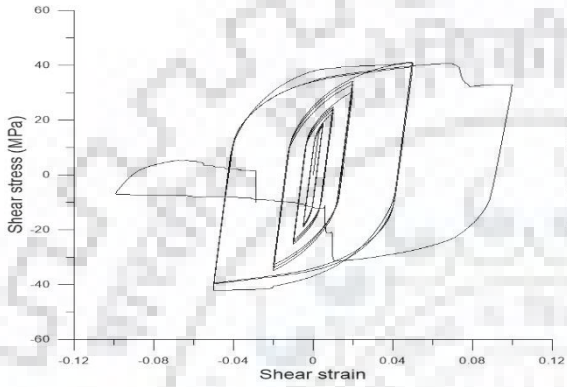

Specimen E1

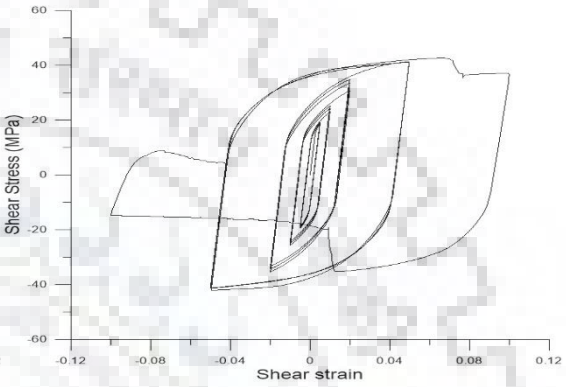

Specimen E2

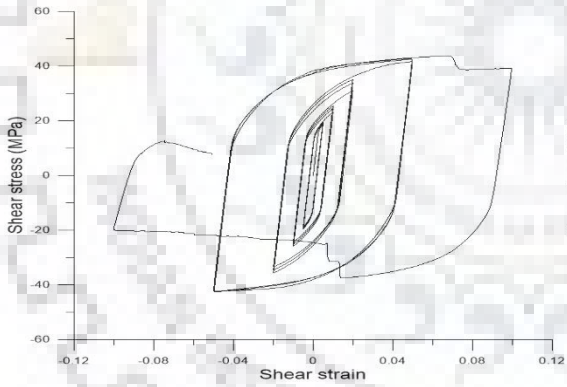

Specimen E3

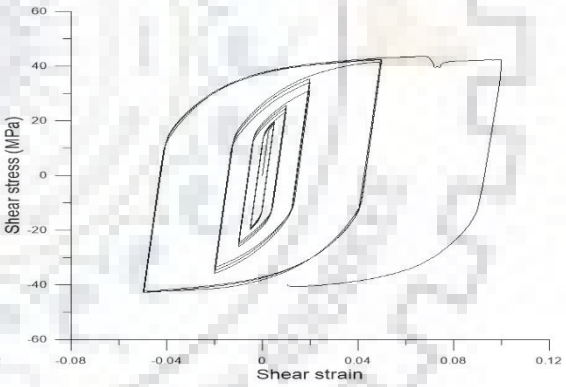

Specimen E4

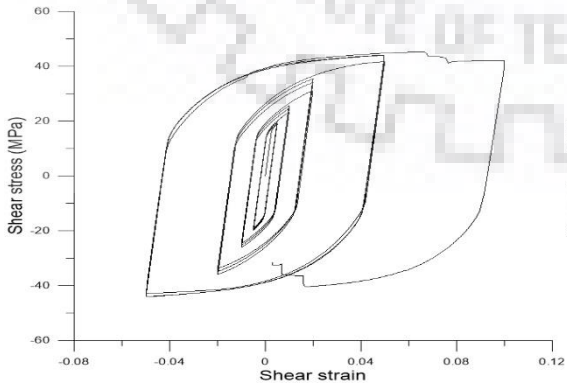

Specimen E5

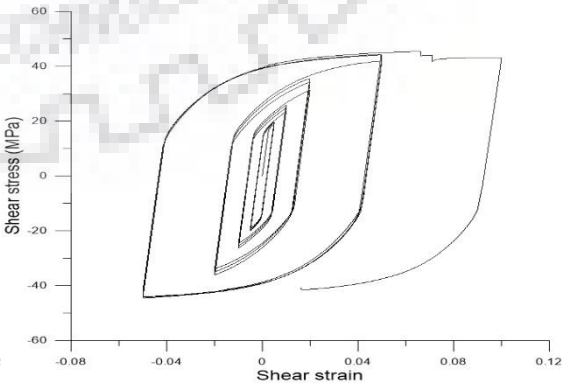

Specimen E6

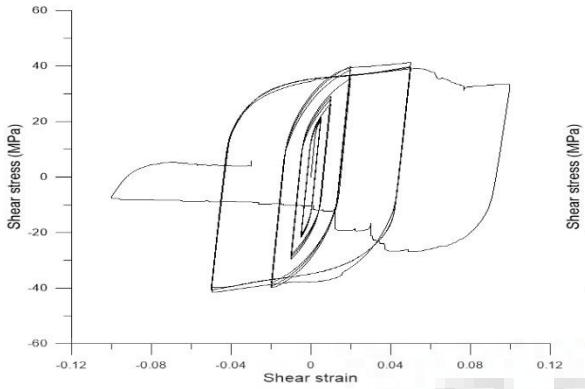

Specimen F1

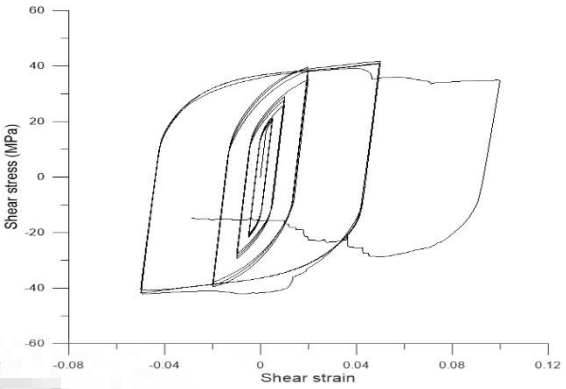

Specimen F2

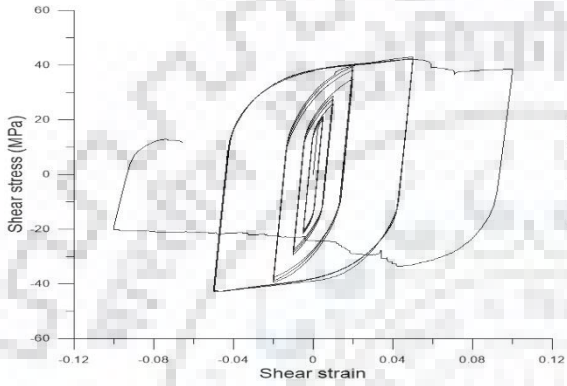

Specimen F3

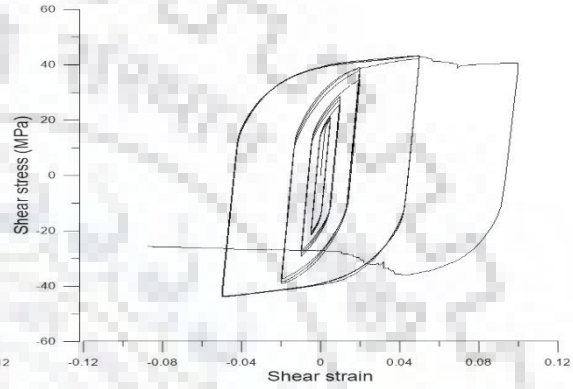

Specimen F4

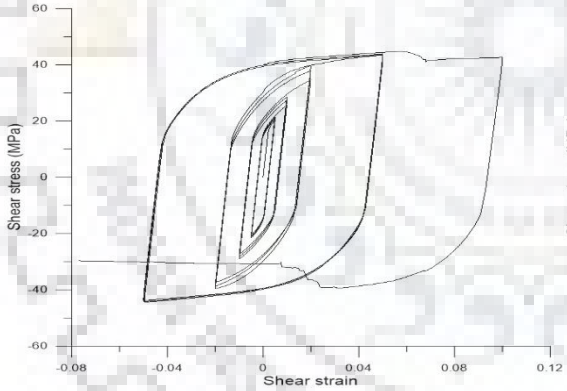

Specimen F5

Specimen F6

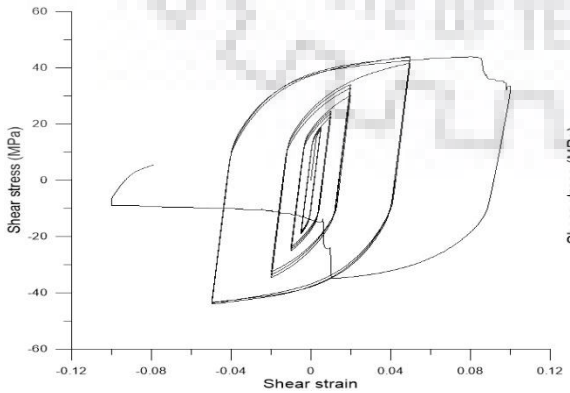

Specimen G1

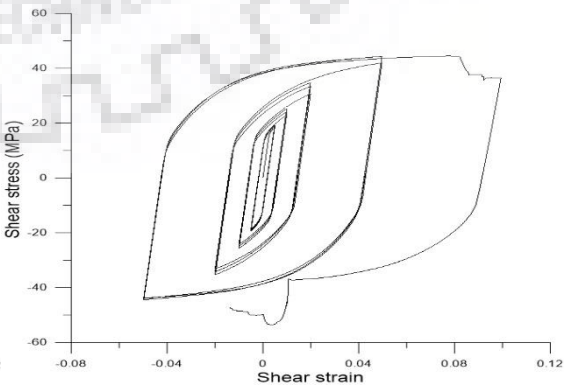

Specimen G2

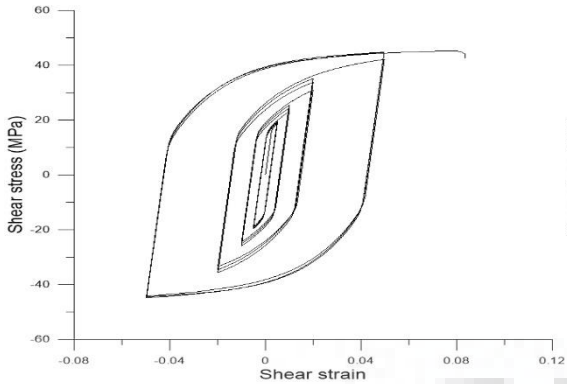

Specimen G3

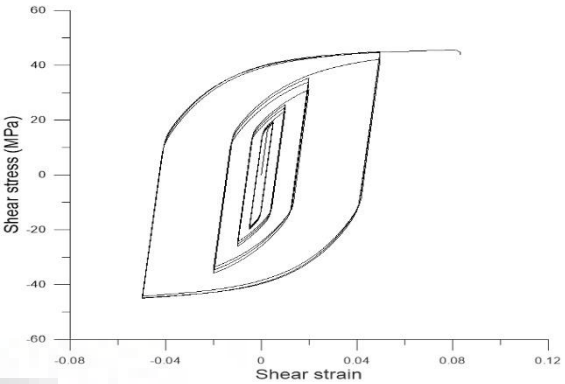

Specimen G4

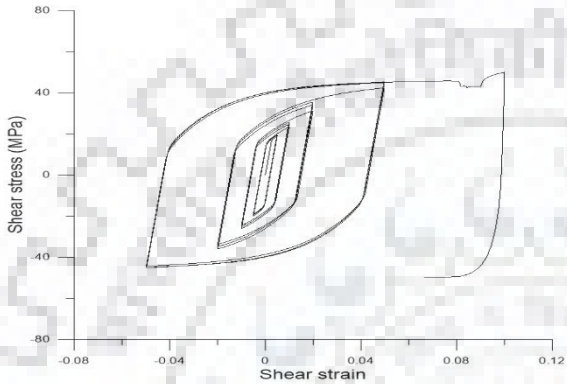

Specimen G5

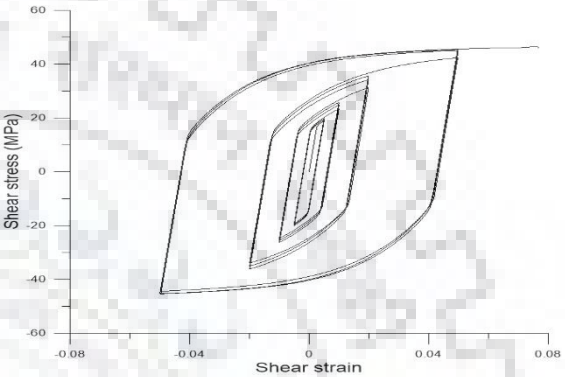

Specimen G6

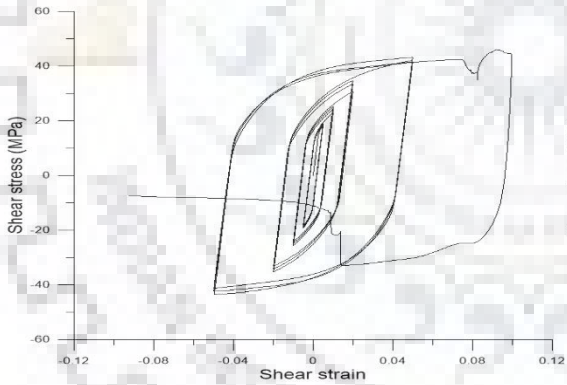

Specimen H1

Specimen H2

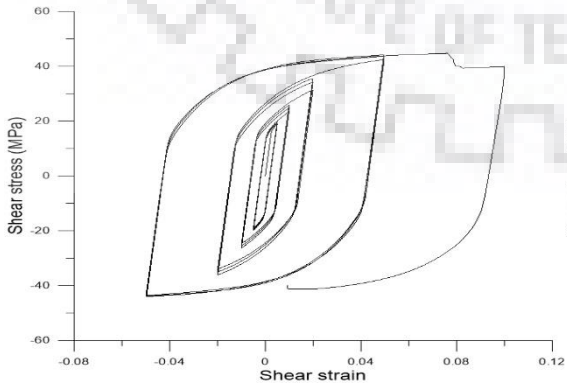

Specimen H3

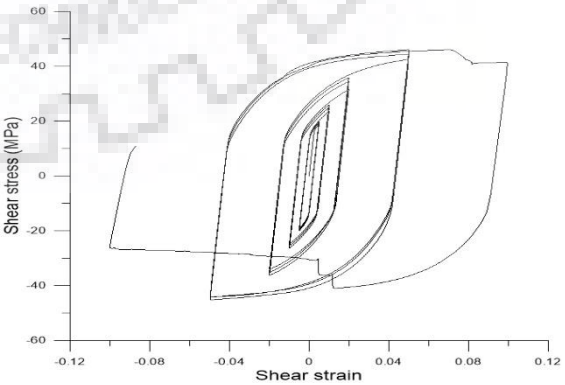

Specimen H4

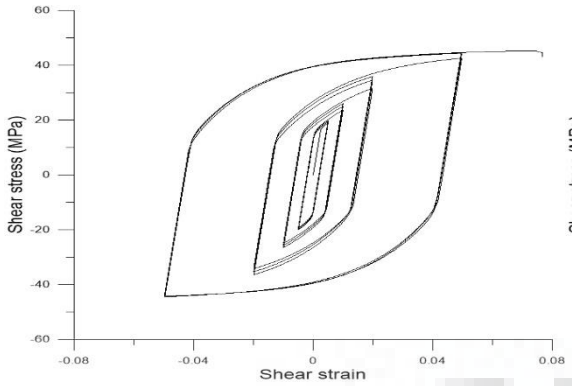

Specimen H5

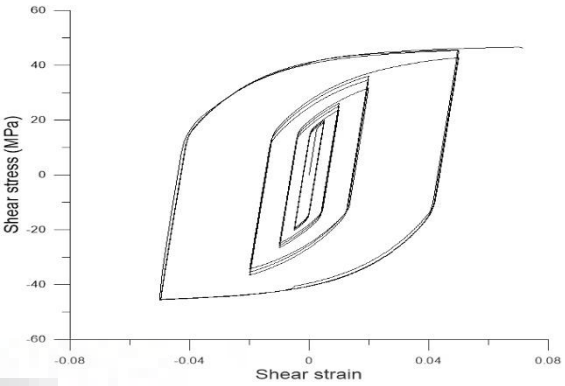

Specimen H6

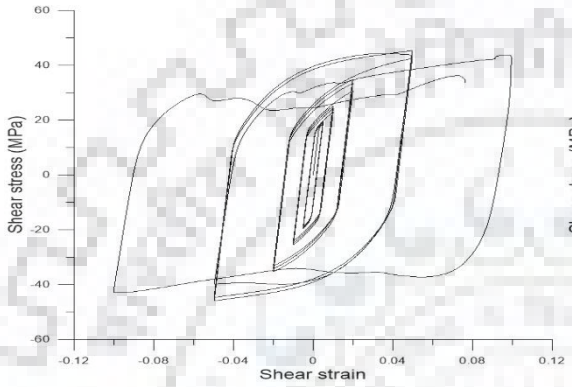

Specimen I1

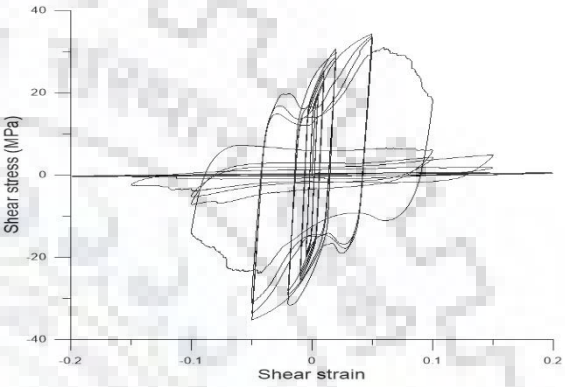

Specimen I3

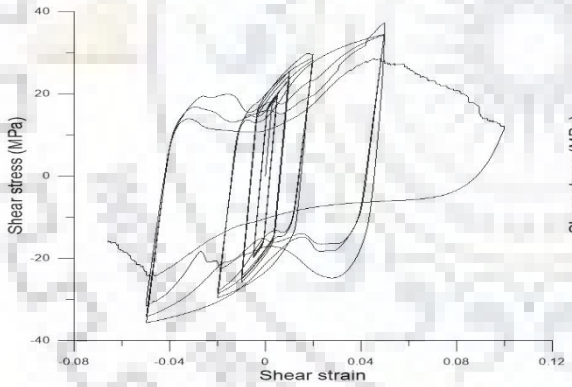

Specimen I4

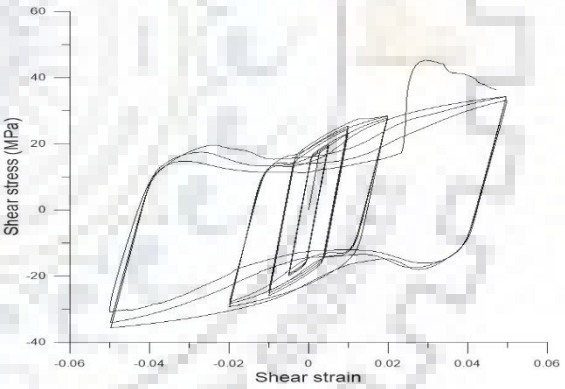

Specimen I5

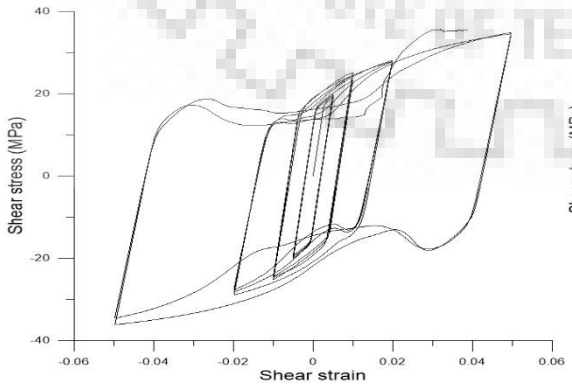

Specimen I6

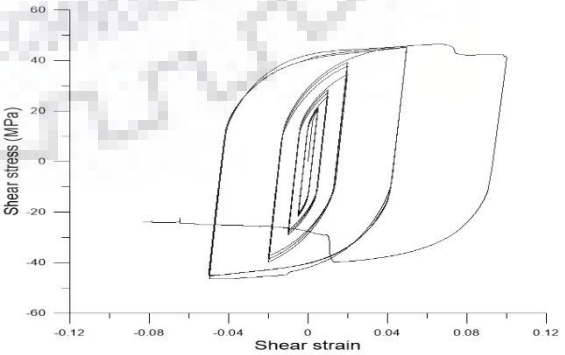

Specimen J1

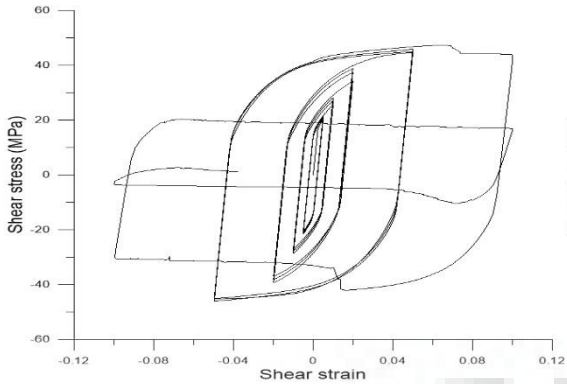

Specimen J2

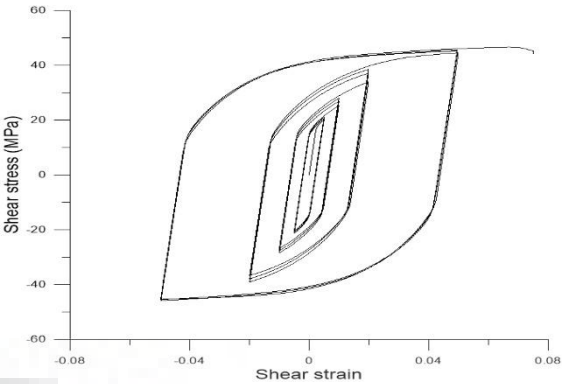

Specimen J3

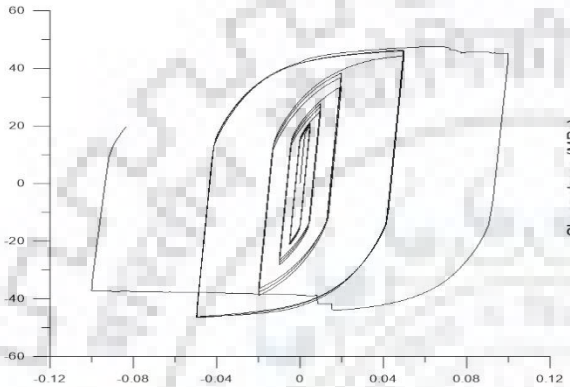

Specimen J4

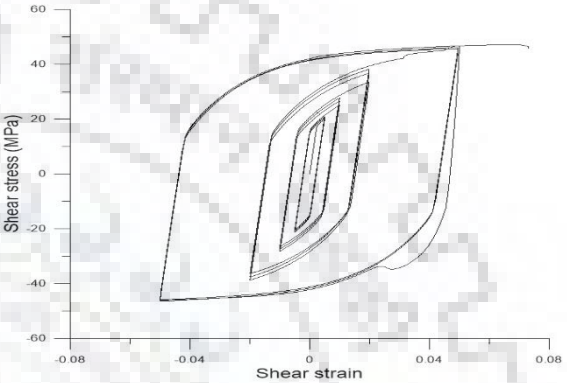

Specimen J5

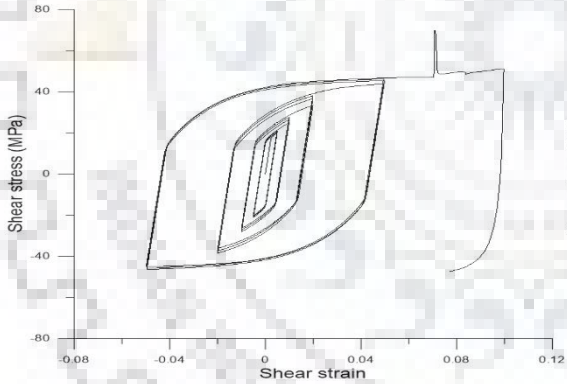

Specimen J6

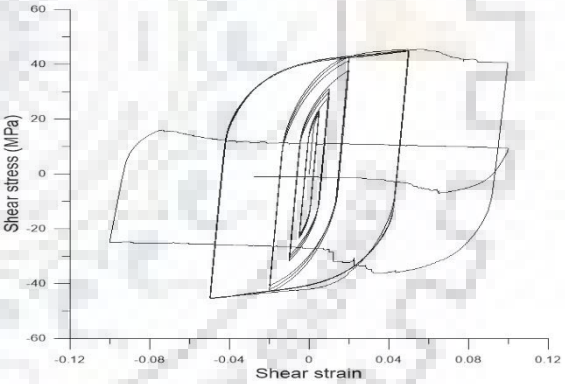

Specimen K1

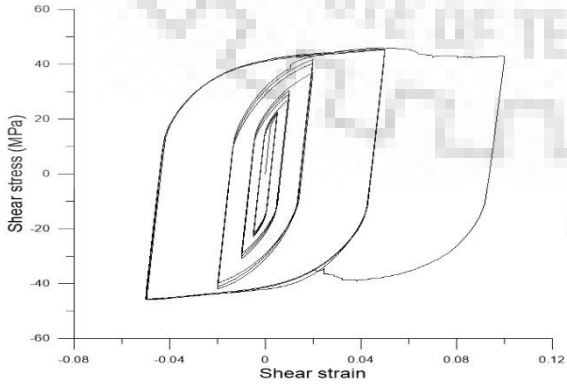

Specimen K2

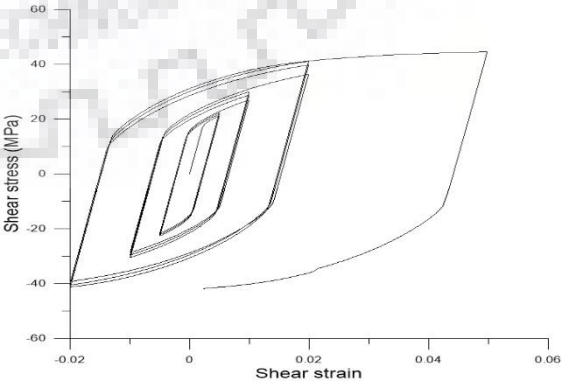

Specimen K3

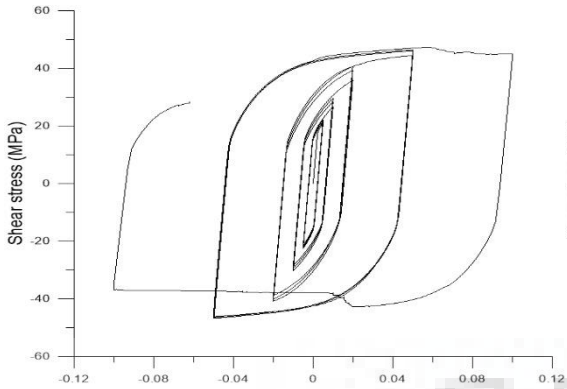

Specimen K4

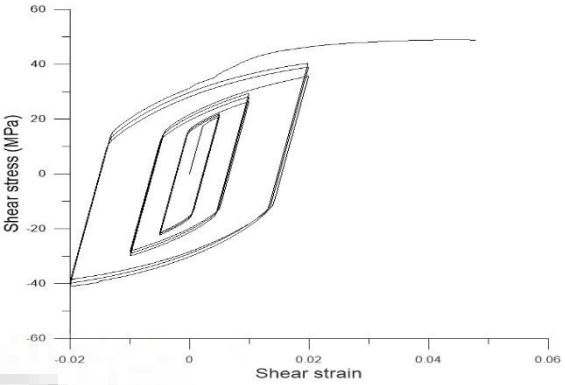

Specimen K5

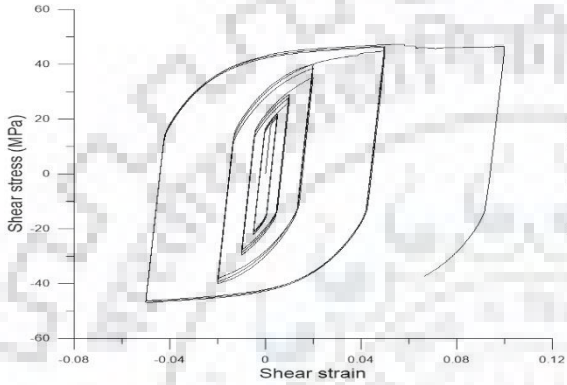

Specimen K6

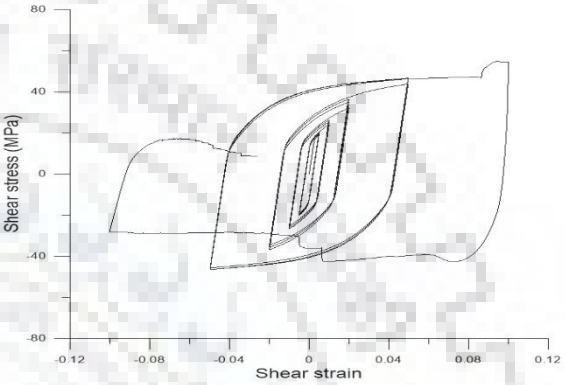

Specimen L1

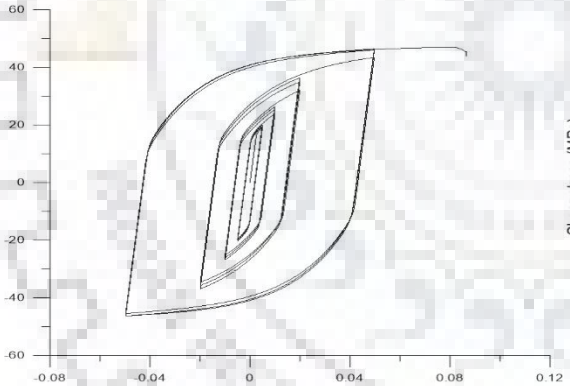

Specimen L2

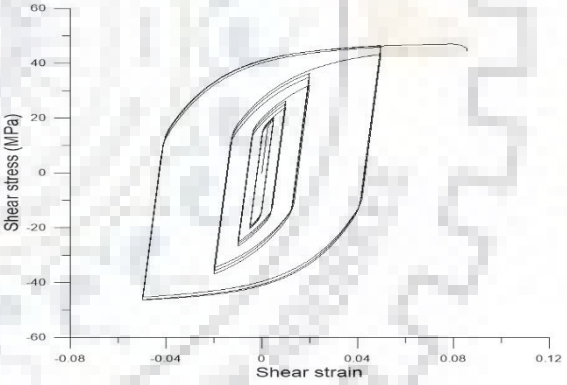

Specimen L3

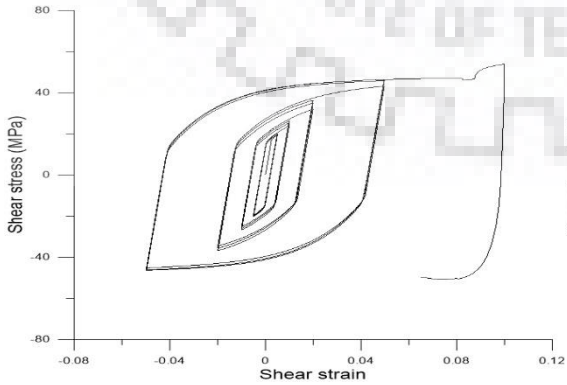

Specimen L4

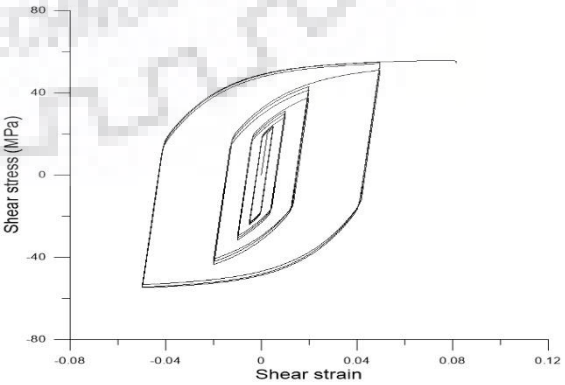

Specimen L5

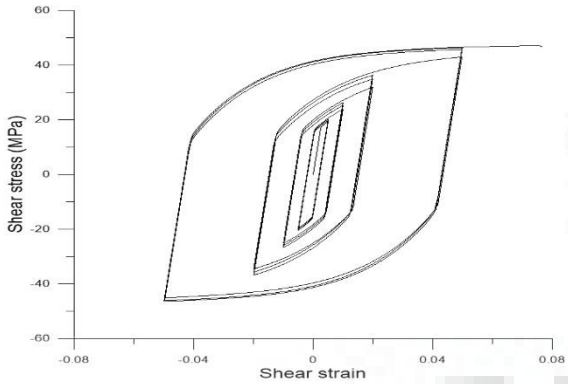

Specimen L6

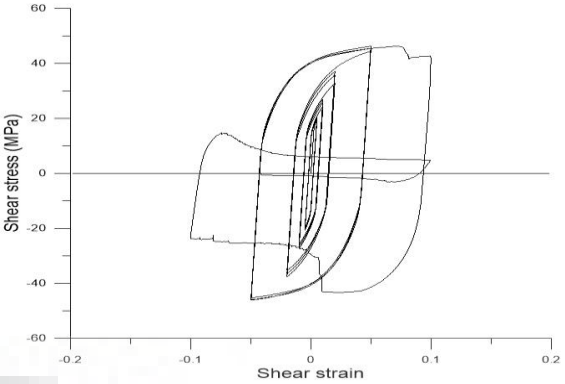

Specimen M1

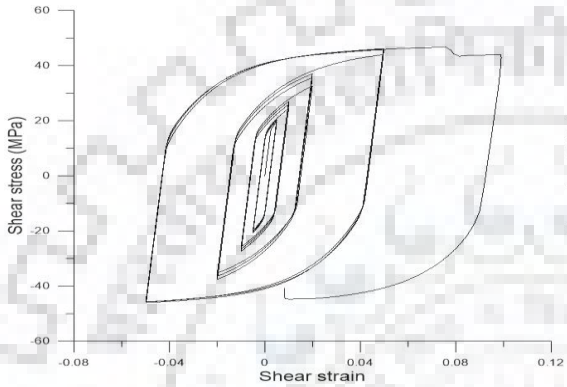

Specimen M2

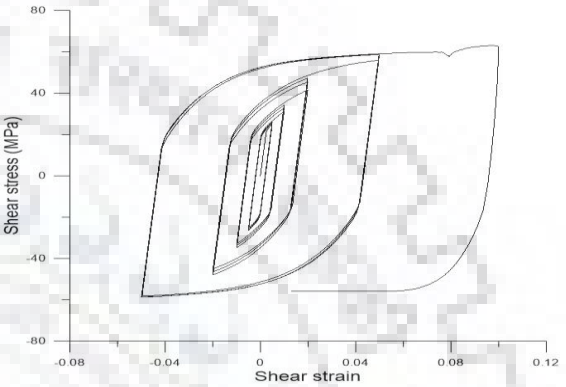

Specimen M3

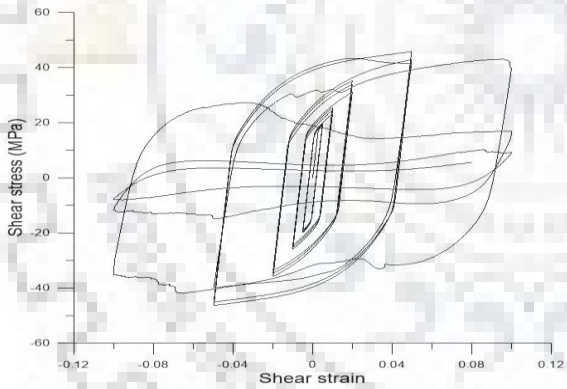

Specimen N1

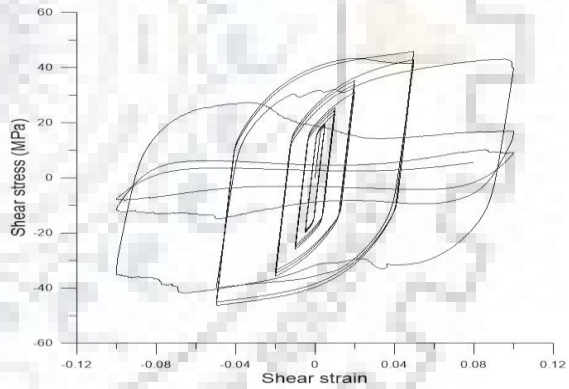

Specimen N2

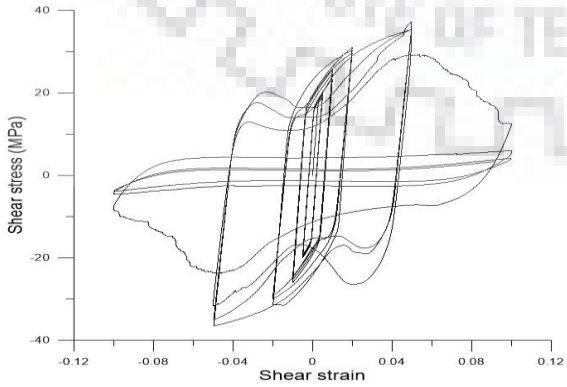

Specimen N3

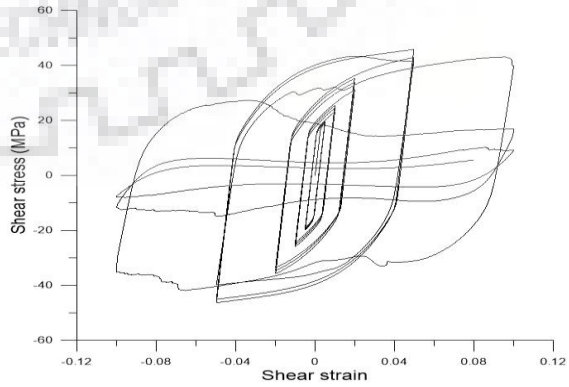

Specimen N4

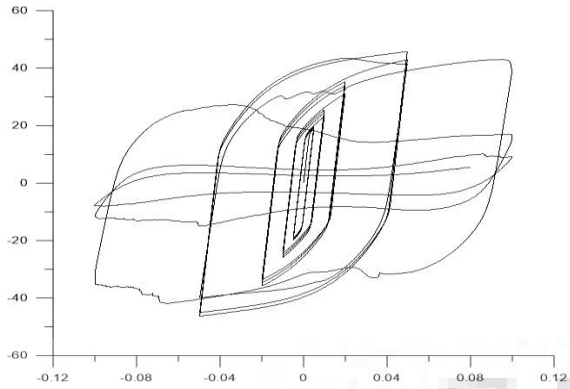

Specimen O1

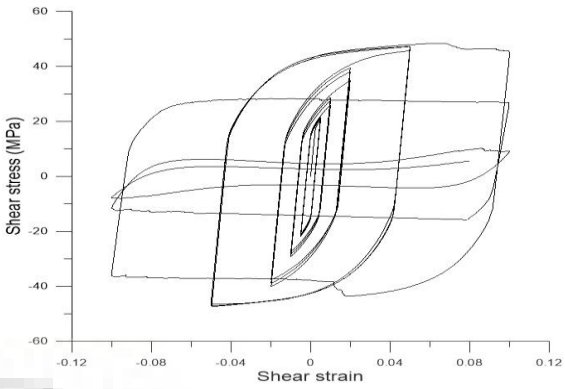

Specimen O2

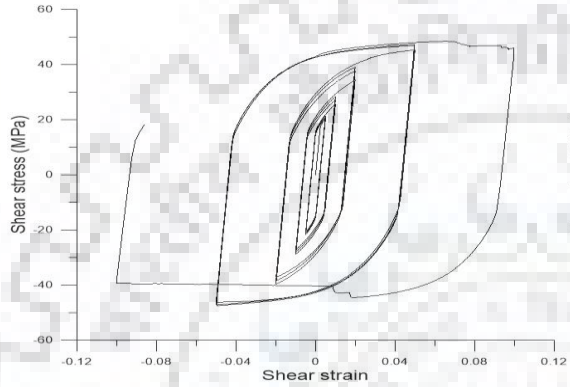

Specimen O3

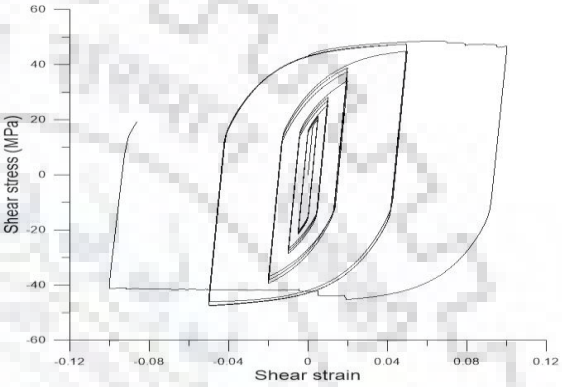

Specimen O4

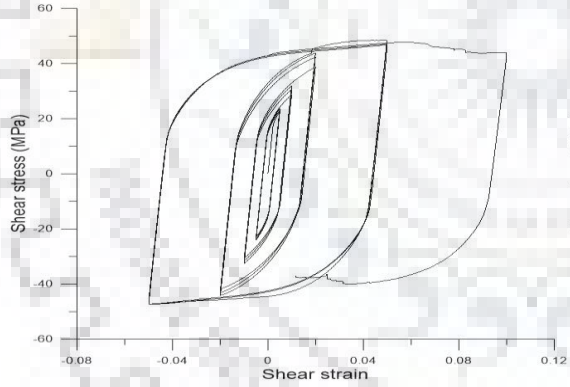

Specimen P1

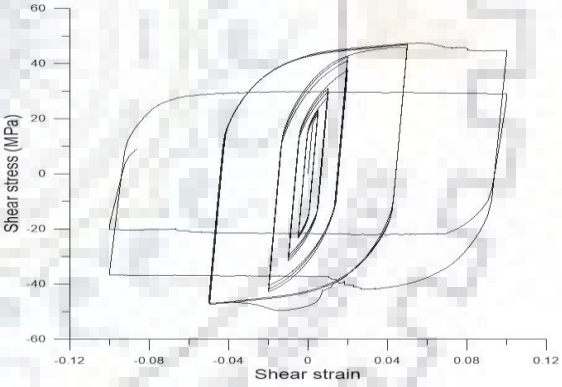

Specimen P2

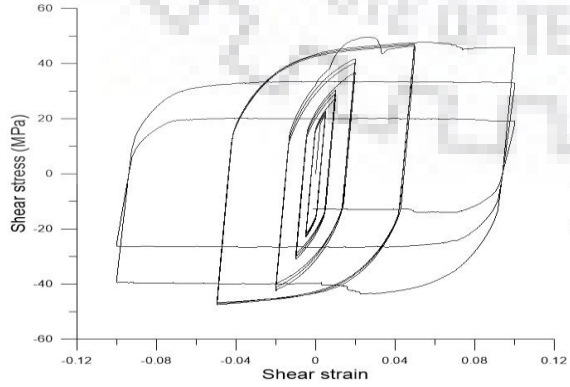

Specimen P3

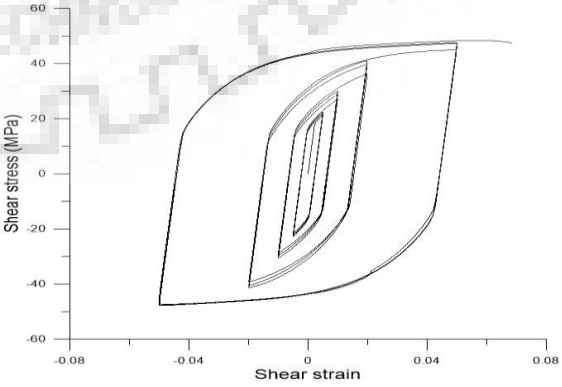

Specimen P4

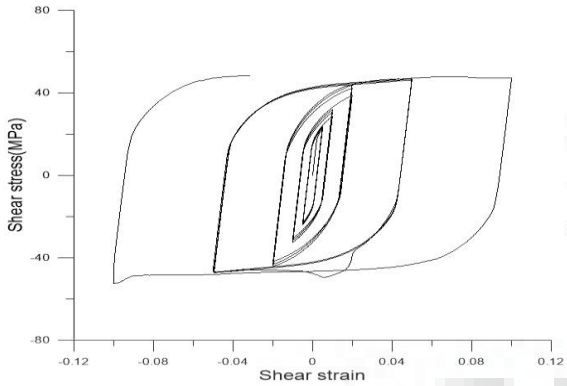

Specimen P1 0.82

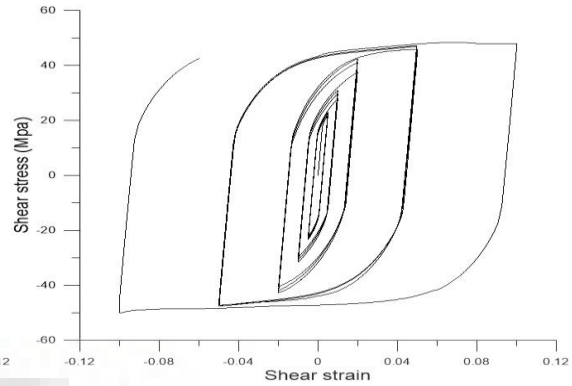

Specimen P2 0.82

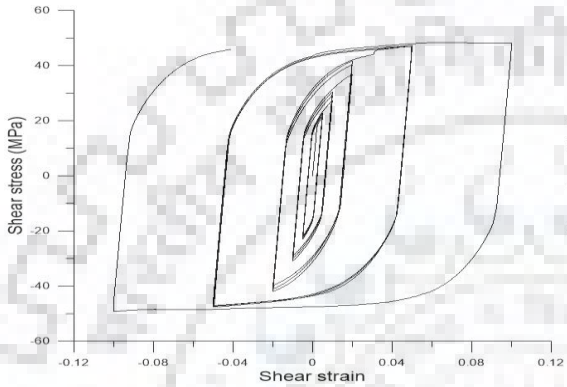

Specimen P3 0.82

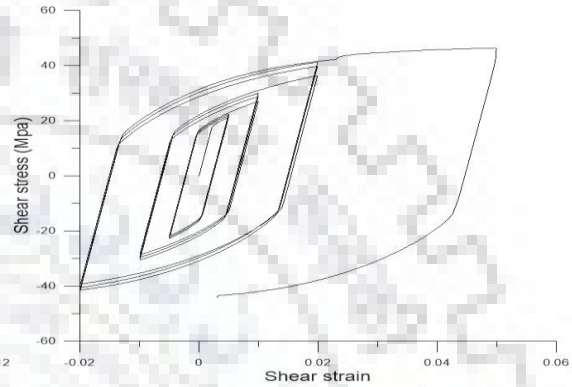

Specimen P4 0.82]

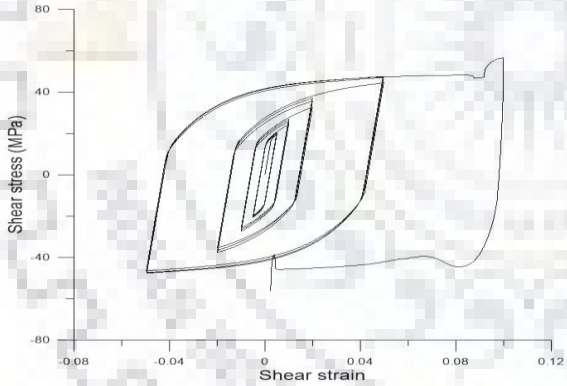

Specimen Q1

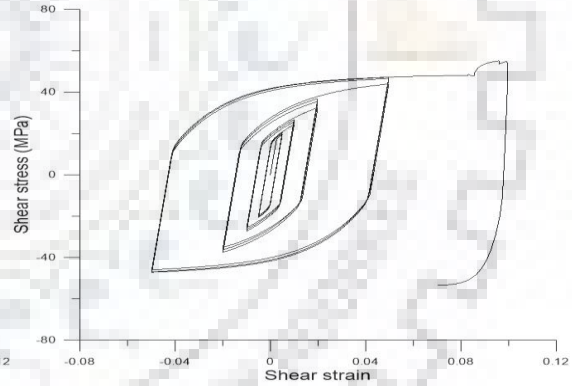

Specimen Q2

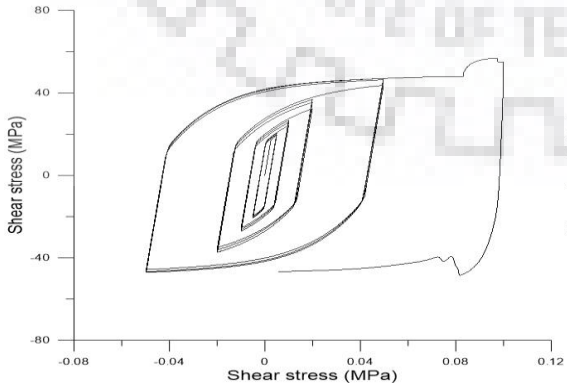

Specimen Q3

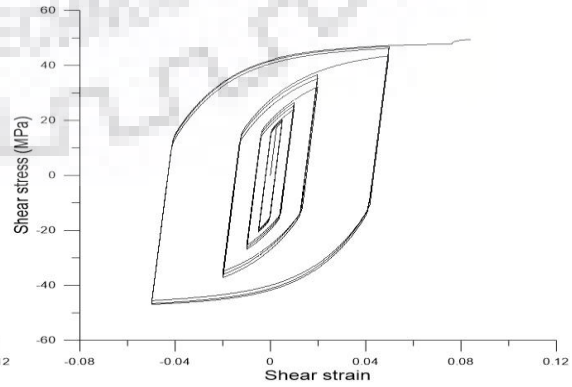

Specimen Q4

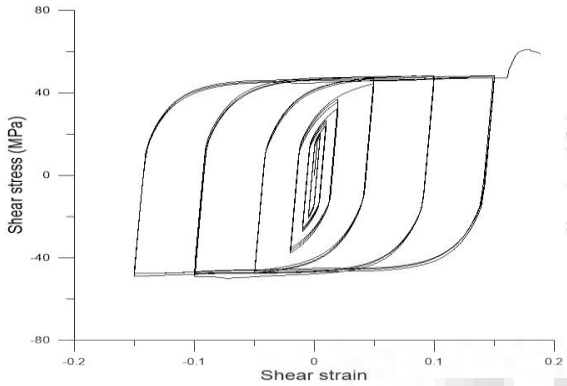

Specimen Q1 0.82

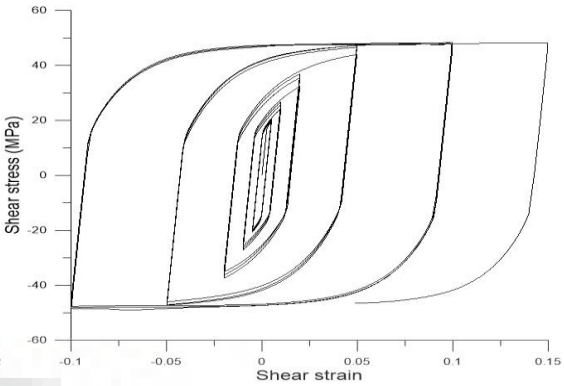

Specimen Q2 0.82

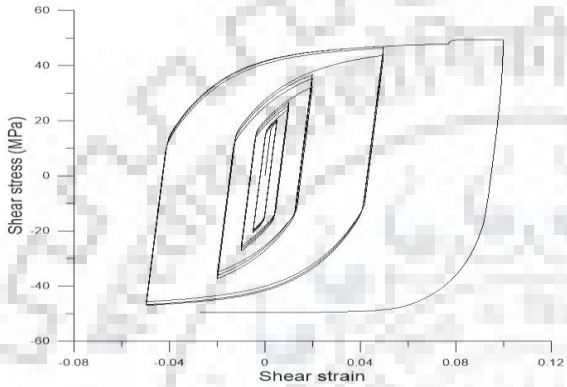

Specimen Q3 0.82

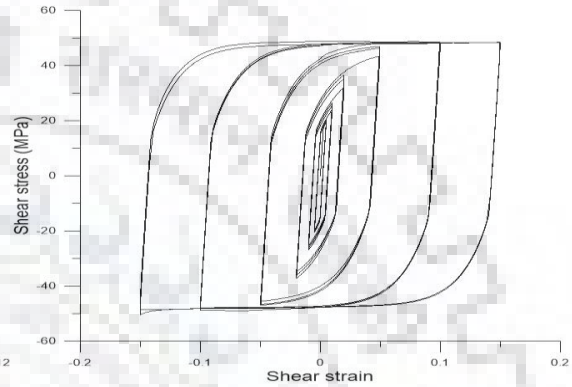

Specimen Q4 0.82

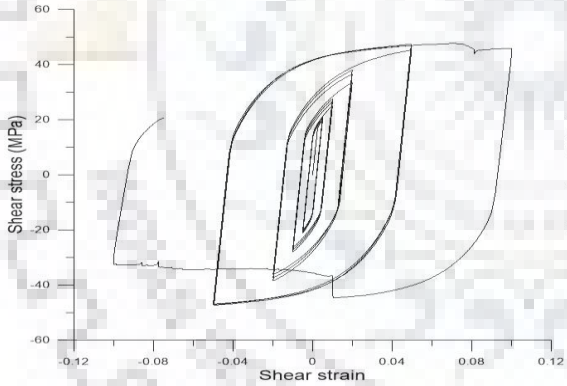

Specimen R1

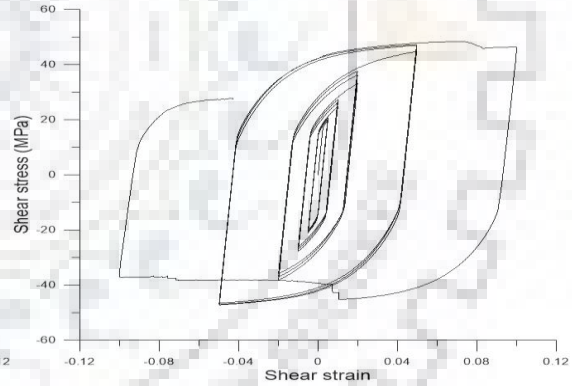

Specimen R2

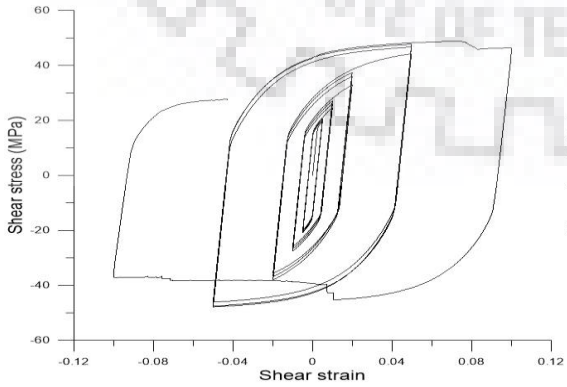

Specimen R3

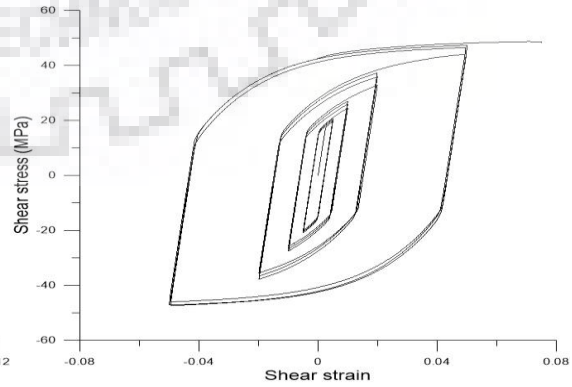

Specimen R4

APPENDIX-2

Curves between the energy calculated from the hysteresis curves and the increment number

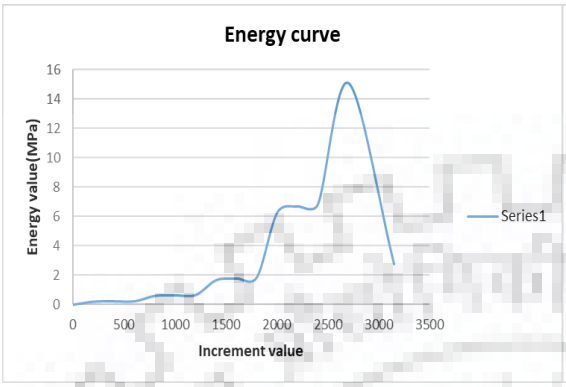

Specimen A1

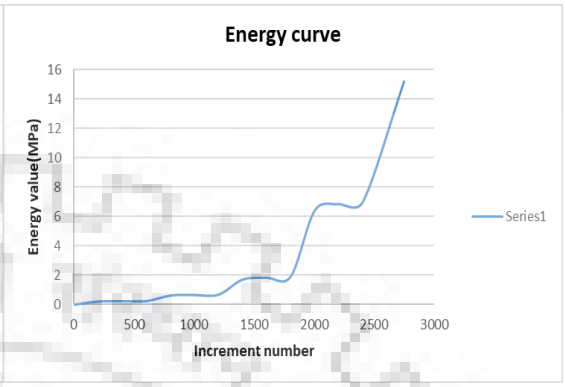

Specimen A2

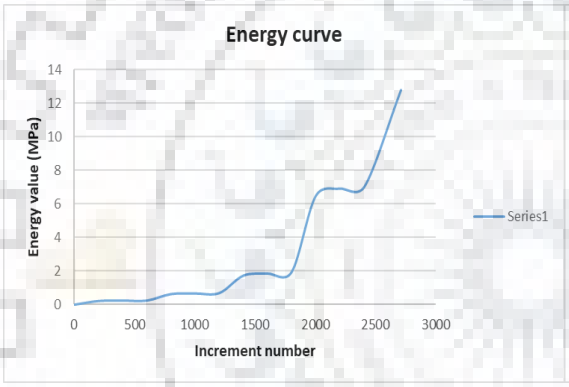

Specimen A3

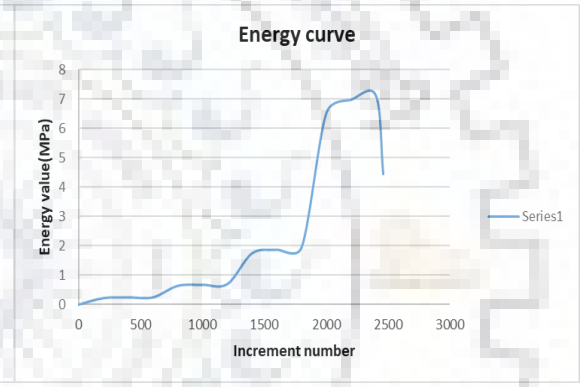

Specimen A4

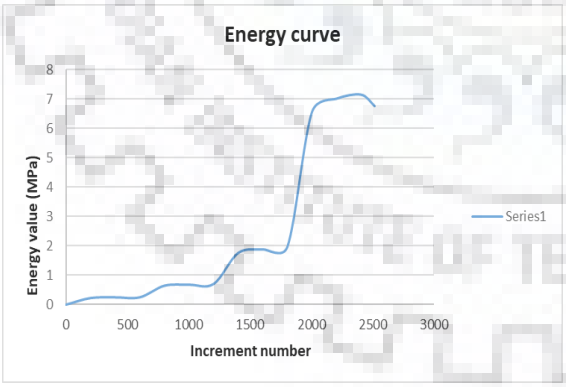

Specimen A5

APPENDIX-3

The following curves show us the key design points. These are the backbone curves of the specimens showing the variation of the extreme points of stress (MPa) with respect to strain.

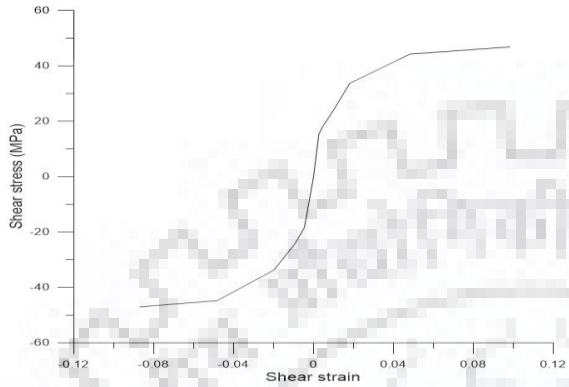

Specimen A1

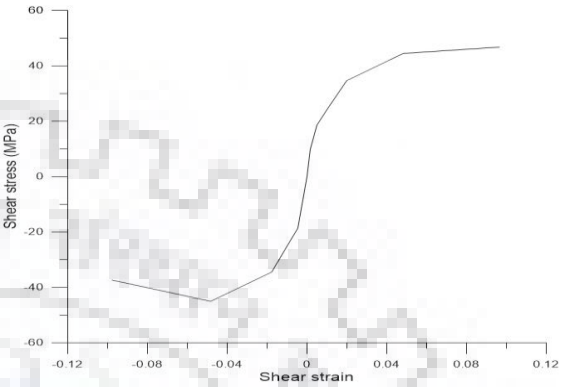

Specimen A2

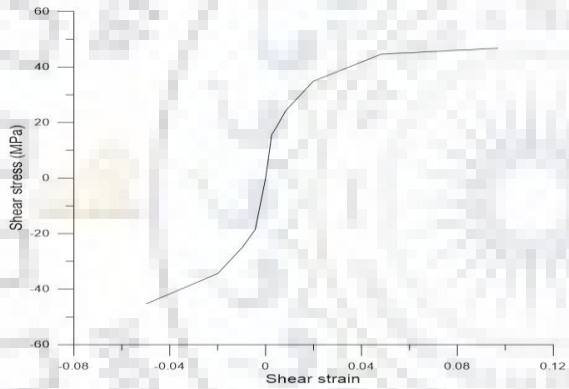

Specimen A3

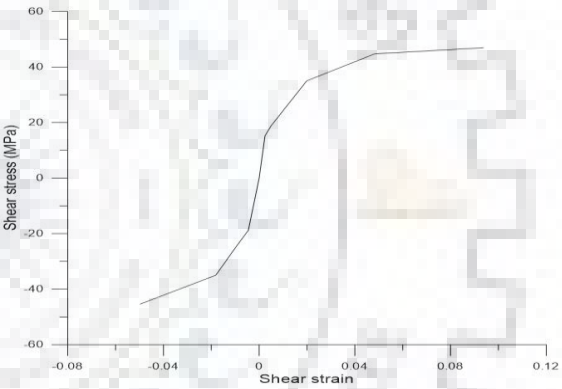

Specimen A4

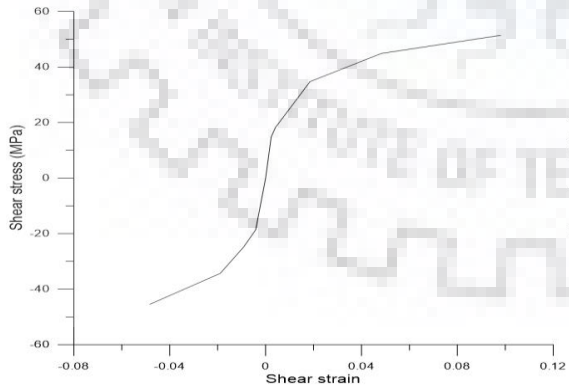

Specimen A5

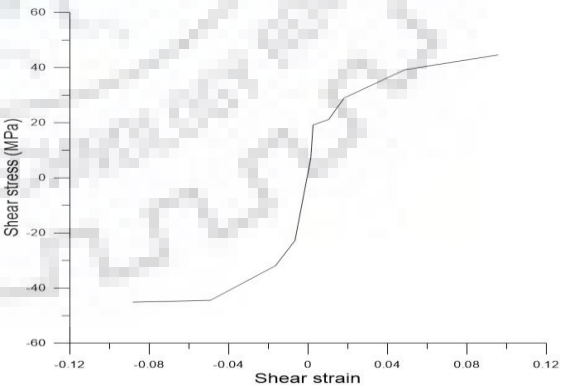

Specimen A6

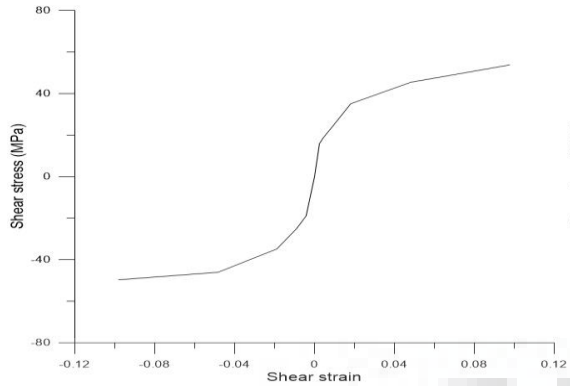

Specimen B1

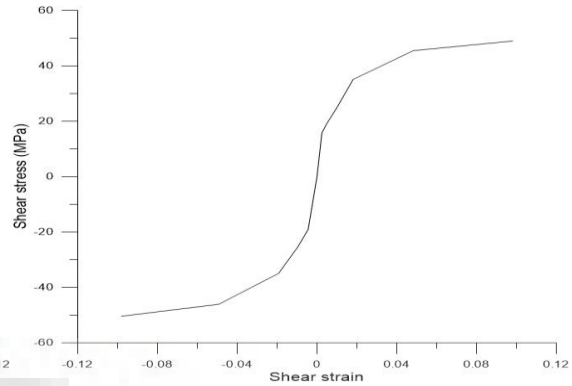

Specimen B2

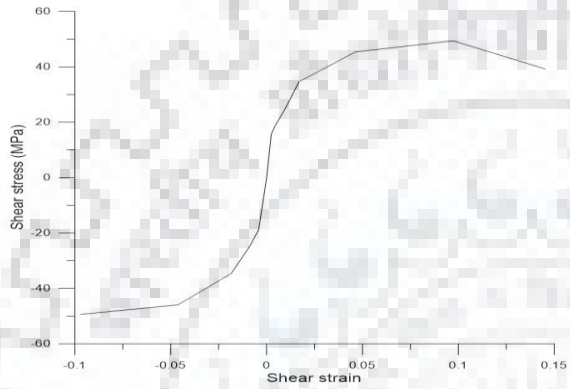

Specimen B3

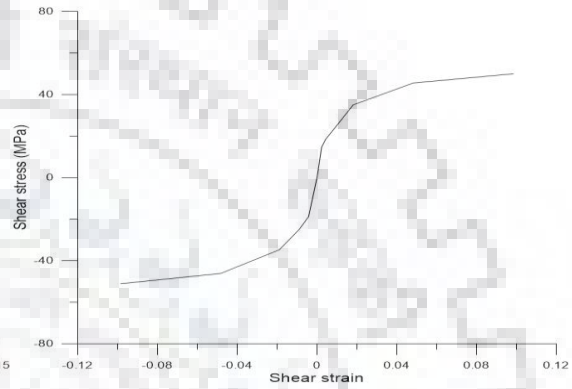

Specimen B4

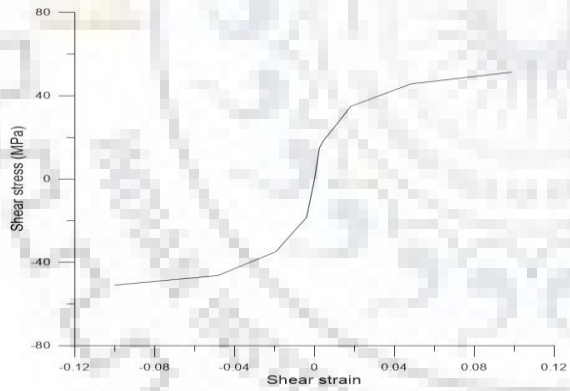

Specimen B5

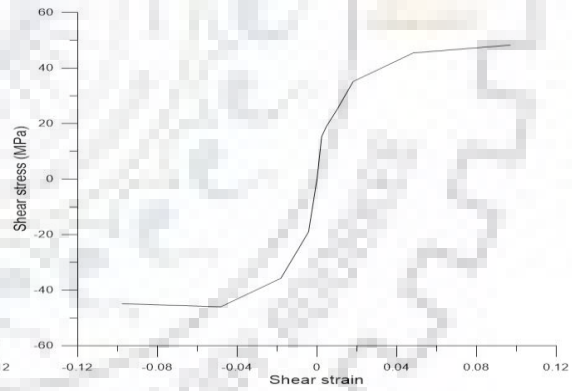

Specimen B6

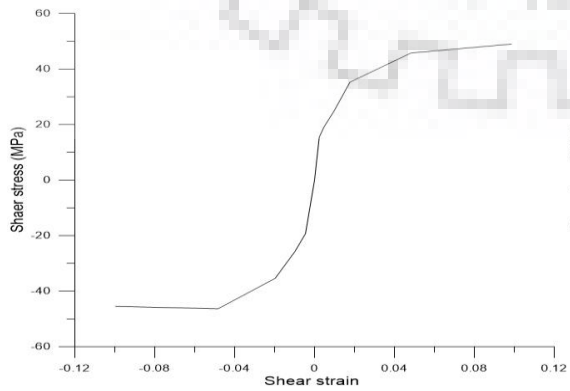

Specimen C1

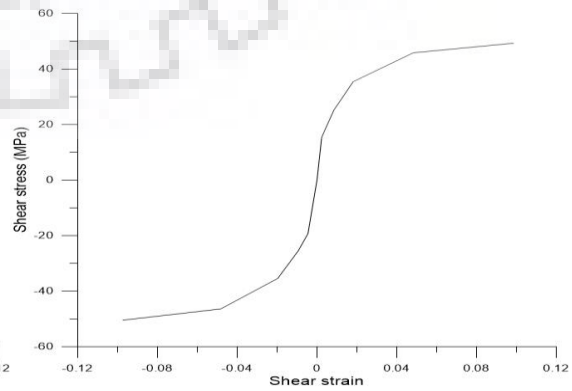

Specimen C2

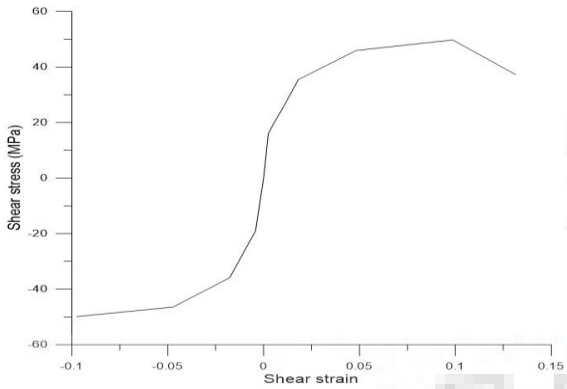

Specimen C3

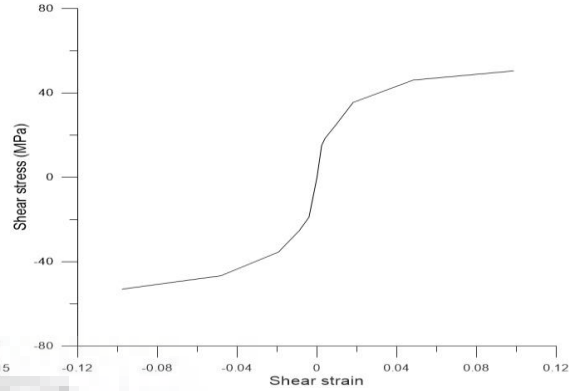

Specimen C4

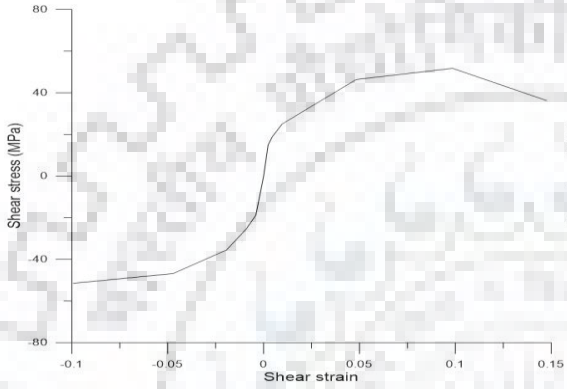

Specimen C5

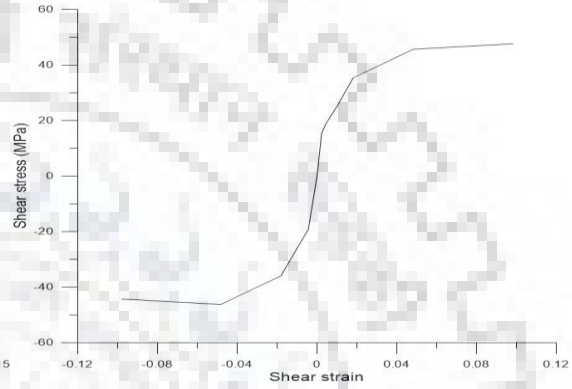

Specimen C6

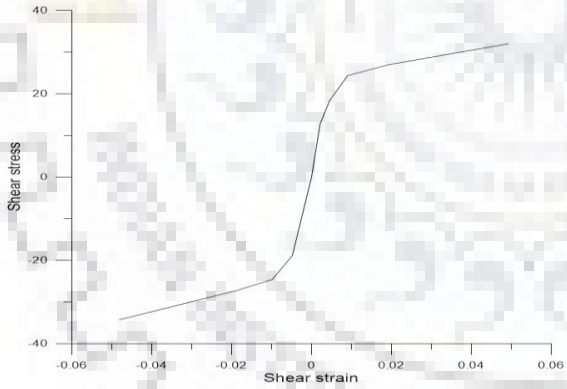

Specimen D1

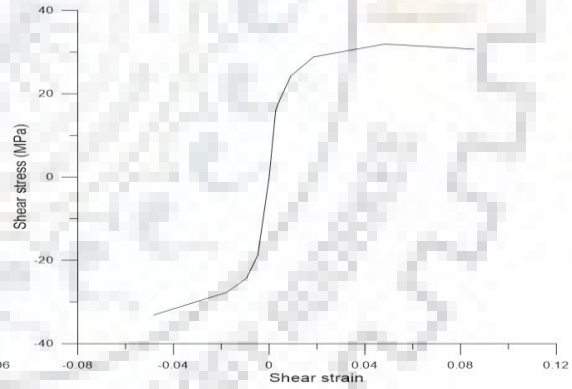

Specimen D2

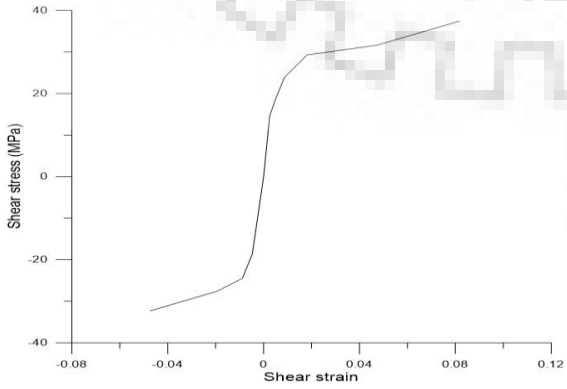

Specimen D3

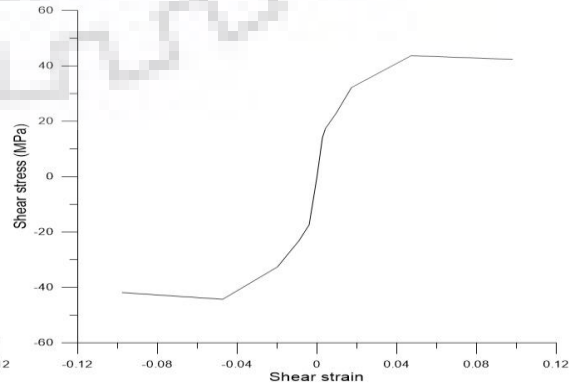

Specimen D4

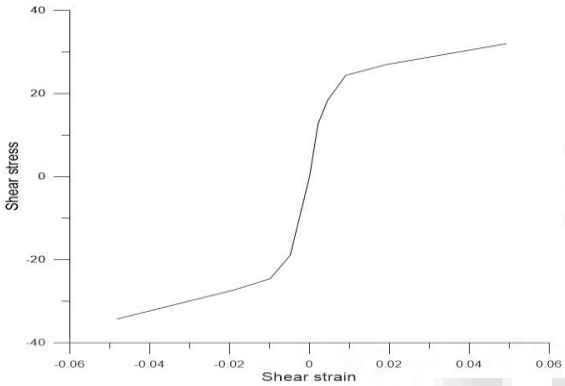

Specimen D5

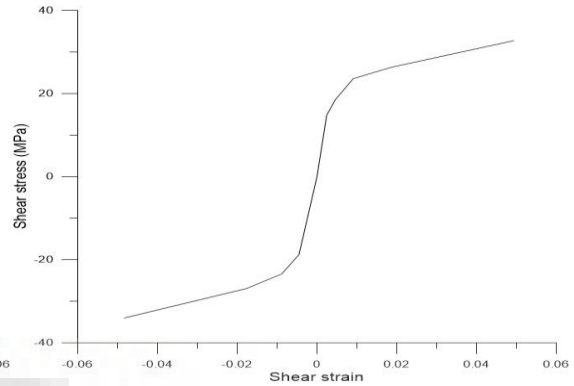

Specimen D6